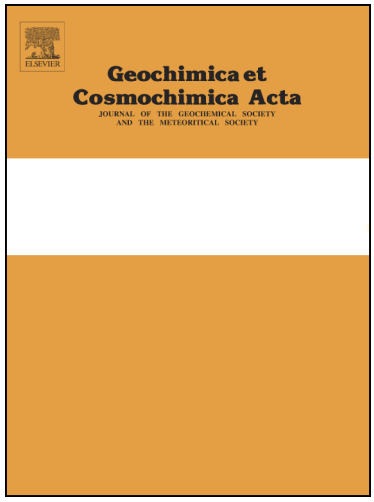

A self-consistent optimization of multicomponent solution properties: *ab initio* molecular dynamic simulations and the MgO-SiO_2 miscibility gap under pressure

Jean-Philippe Harvey, Aïmen E. Gheribi, Paul D. Asimow

PII: S0016-7037(15)00197-0
DOI: http://dx.doi.org/10.1016/j.gca.2015.04.004
Reference: GCA 9210

To appear in: *Geochimica et Cosmochimica Acta*

Received Date: 15 August 2014
Accepted Date: 2 April 2015

Please cite this article as: Harvey, J-P., Gheribi, A.E., Asimow, P.D., A self-consistent optimization of multicomponent solution properties: *ab initio* molecular dynamic simulations and the MgO-SiO_2 miscibility gap under pressure, *Geochimica et Cosmochimica Acta* (2015), doi: http://dx.doi.org/10.1016/j.gca.2015.04.004

A self-consistent optimization of multicomponent solution properties: *ab initio* molecular dynamic simulations and the MgO-SiO_2 miscibility gap under pressure

Jean-Philippe Harvey[1,*], Aïmen E. Gheribi[2] and Paul D. Asimow[1]

[1]Division of Geological and Planetary Sciences, California Institute of Technology, Pasadena CA 91125 USA

[2]Center for Research in Computational Thermochemistry, Department of Chemical Engineering, École Polytechnique de Montréal, C.P. 6079, Station Downtown, Montréal (Québec), CANADA, H3C 3A7

[*] jean-philippe.harvey@polymtl.ca

ABSTRACT

We propose a new approach to parameterizing the Gibbs energy of a multicomponent solution as a function of temperature, pressure and composition. It uses the quasichemical model in the second nearest neighbour approximation and considers both a polynomial representation (for low pressure) and an exponential decay representation (for moderate-to-high pressure) of the excess molar volume v^{xs} to extend thermodynamic behaviour to elevated pressure. This approach differs from previous configuration-independent regular or associated solution-type models of multicomponent silicate liquids at elevated pressure and can account for any structural or short-range order data that may be available. A simultaneous least squares fit of the molar volume and the molar enthalpy of mixing data obtained from First Principles Molecular Dynamics (FPMD) simulations at various pressures enables complete parameterization of the excess thermodynamic properties of the solution. Together with consistently optimized properties of coexisting solids, this enables prediction of pressure-temperature-composition phase diagrams associated with melting. Although the method is extensible to natural multicomponent systems, we apply the procedure as a first test case to the important planetary model system MgO-SiO_2 using FPMD data found in the literature. One key result of this optimization, which depends only on the derived excess properties of the liquid phase, is that the consolute temperature of the SiO_2-rich miscibility gap is predicted to decrease with increasing pressure. This appears to be in

disagreement with available experimental constraints and suggests possible thermodynamic inconsistency between FPMD data and experimental phase equilibrium data in the 0-5 GPa pressure range. We propose a new thermodynamic consistency criterion relating the signs of v^{xs} and other excess properties and discuss the need for precise calculations of derivatives of excess properties. Finally, the potential reappearance of the miscibility gap in the MgO-SiO_2 system above 5 GPa is discussed in light of this work.

I. Introduction

Our ability to describe the range of evolutionary pathways for terrestrial planets and to identify, through interpretation of available data, the particular pathway that the Earth followed depends on our understanding of the thermo-physical properties of Earth materials subjected to a wide range of conditions. In particular, multi-component liquid and solid solutions of oxides, metals and silicates are complex phases whose behavior at elevated pressure (P) and temperature (T) can, at best, be characterized experimentally only at sparsely sampled compositions and (P, T) points. This is one reason that there has been a historical divide between the relatively coarse, configuration-independent models of liquid solutions adopted in geochemistry — where high-pressure experimental constraints are few and the refined (Ghiorso and Sack, 1995; Bottinga and Weill, 1970), parameter-rich, configuration-dependent models preferred in ambient pressure materials science — where data are densely sampled and abundant (Pelton et al., 2000). The continuing advances in numerical tools such as First Principles Molecular Dynamics (FPMD) simulations, though, should eventually provide the densely sampled data on both macroscopic and microscopic properties needed to make progress in multicomponent solution models for high-pressure geochemistry. Applying such simulations, however, often requires derived results obtained by fitting or interpolating the simulation data. The accuracy of the fitting and interpolation method and the accuracy of the simulations themselves then both contribute to uncertainties in this approach. It is our purpose in this contribution to introduce a fully self-consistent scheme for interpolation of multi-component FPMD results extending to high pressure and to discuss the advantages of this approach compared to previous methods. We then attempt a first test case by applying it to the only internally consistent set of FPMD calculations of a geochemically important model system of which we are aware, the MgO-SiO_2 simulation data of de Koker *et al.* (2013). We consider the differences between the inferences drawn from our new

interpolation and the interpolation scheme of de Koker *et al.* (2013); test whether the resulting phase diagrams match available experimental constraints; and speculate whether the disagreements might arise from the experiments, the simulations, or the interpolation schemes.

The particular feature and system that we choose to focus on is the asymmetrical equilibrium miscibility gap in the liquid phase of the MgO-SiO_2 binary system. This binary is both an essential step towards a full understanding of the mantles of terrestrial planets, as these are the two major oxides that dominate the overall compositions, and an important test case of the capabilities of the method, because a comprehensive set of simulations have already been done (de Koker et al., 2013) and substantial experimental data are available to constrain some aspects of the phase diagram and to test the prediction of other aspects. The miscibility gap was originally measured by Ol'shanskii (1951) and Hageman and Oonk (1986) and more recently by Hudon *et al.* (2004, 2005). The miscibility gap is a useful feature to focus on because its accurate prediction provides a very sensitive test of the ability of any modeling method to capture the compositional dependence of the excess Gibbs energy of the liquid relative to the pure end members. By 5 GPa, the rising liquidus surface overtakes the miscibility gap and it disappears from the equilibrium phase diagram, as found experimentally by Dalton and Presnall (1997). The flat shape and upwards concavity of the SiO_2 liquidus in this region is, however, a clear indication that the repulsive energetic tendency of the melt is still present under these equilibrium conditions and suggests the consolute point is not far below the liquidus. The question that arises is whether the miscibility gap may reappear at higher pressure. If it does, it implies that non-ideal mixing relations persist or even increase with increasing pressure. Such behaviour might be surprising, since immiscibility is often associated with mixing of unlike species and, with increasing pressure, the SiO_2 component in silicate liquids shifts from four-coordinated, network-forming behaviour towards six-coordinated structures nominally more similar to those adopted by the MgO component. While actual formation of liquids silicic enough to encounter this miscibility gap (or its multicomponent extension) in the Earth is speculative, we feel that examination of the MgO-SiO_2 miscibility gap provides basic insight into the energetics of liquid solutions, the relationship between microstructure and macroscopic thermodynamics, and the internal consistency of various modeling and fitting approaches. In this work we refrain from presenting complete predicted phase diagrams at high pressure that depend

on the assessment of high-pressure solid phases as well as the liquid solution, in order to focus our discussion on the accuracy of the liquid solution model itself.

As pointed out by de Koker *et al.* (2013), FPMD simulations can allow the definition of the Gibbs energy of geologically important multicomponent solutions for a large range of pressure and temperature, but this requires a statistical analysis and post-treatment of the evolution of internal energy and pressure data obtained in different thermodynamic ensembles (canonical ensemble, micro-canonical ensemble, etc.). We emphasize that the miscibility gap, in particular, is sensitive to the excess Gibbs energy of the solution relative to the end members, and so it is important to focus on how this excess quantity is derived. To model MgO-SiO_2 binary liquids, de Koker *et al.* (2013) proceeded through several steps. (a) They carried out canonical ensemble (NVT) FPMD simulations at several discretely sampled compositions, temperatures, and volumes. (b) They fit the simulation results for each discrete melt composition to a self-consistent formulation of the Helmholtz free energy involving ideal gas, excess, and electronic contributions (de Koker and Stixrude, 2009) in which the excess term is a polynomial expansion in dimensionless temperature and in a volume parameter akin to finite-strain (Davies, 1973), followed by a Legendre transform to assess the Gibbs energy function $G(P,T)$ of each discrete melt composition. Finally (c), they obtained the composition-dependent function $G(P,T,X)$, the excess properties of the liquid solution, and computed phase diagrams by interpolating empirically among the Gibbs energy functions of each composition using an asymmetric regular solution model and by incorporating models of the solid phases and constraints from the 1 atm phase diagram.

(a) Supercomputers are still limited in the number of FPMD simulations which can be done in order to generate, within a reasonable amount of time, a useful set of thermo-physical data. For that reason, simulations belonging to the canonical ensemble (NVT) are most often used for exploring the thermodynamic behaviour of solutions, rather than more laborious simulations performed in the isothermal-isobaric (NPT) ensemble. In this context, it is important to point out the differences in precision of predictions between those first-order properties that are direct simulation outputs — such as the internal energy, the equilibrium volume, the equilibrium pressure and the equilibrium temperature — and second order properties that are derived from interpolation among these direct simulation outputs. This category includes both

properties defined at constant composition — such as the thermal expansion coefficient, the bulk modulus, the Grüneisen parameter, etc. — and functions of composition such as chemical potential, configurational entropy, excess Gibbs energy, etc.

(b) The direct evaluation of second order thermo-physical parameters from finite differences, statistical fluctuations, or thermodynamic integration of MD simulations is typically subject to large errors due to the technical limitations of simulation time and statistical sampling of the simulations. Hence, in the work of de Koker *et al.* (2013), second order thermo-physical properties at fixed composition are calculated from Maxwell relations applied to a Helmholtz energy model parameterized for each studied composition using internal energy and pressure results. This strategy ensures that all thermo-physical properties are self-consistent for each specific composition.

(c) Compositional systematics of the binary system are obtained by de Koker *et al.* (2013) by then interpolating among the self-consistent Gibbs energy functions fitted to simulation data at each composition. But this approach does not guarantee that the resulting excess properties (referred to pure liquid SiO_2 and MgO) are behaving self-consistently if, for example, different expansion orders are used for different compositions in the system. The question of whether or not the miscibility gap reappears at high pressures, in particular, addresses the precise definition of the excess thermodynamic properties of the melt, not the absolute values of its thermodynamic functions. In this context, the self-consistent definition of compositional derivatives is paramount in predicting the phase diagram.

In this paper, we present a new procedure for optimizing the molar enthalpy of mixing and molar volume data obtained from FPMD simulations at different pressures. This results in a complete set of fully coherent thermo-physical properties of the binary system using classical thermodynamics. The modified quasichemical model, in the second nearest neighbour approximation proposed by Pelton and Blander (1986) and presented in section II of this work, is used to define the thermodynamic properties at 0 GPa as in previous work (Hudon *et al.*, 2005; Wu *et al.*, 1993). Excess thermo-physical properties at higher pressures are predicted by integrating the equation defining the excess volume v^{xs} of the considered single phase. This procedure is applied to the MgO-SiO_2 system using the NVT-FPMD simulation data presented by de Koker *et al.* (2013), and certain features of the phase diagram (in particular, the pressure-

temperature-composition evolution of the miscibility gap) is predicted. The result appears inconsistent with experimental phase diagrams and this may point to shortcomings of current-generation FPMD simulations themselves as a basis for constructing a thermodynamic model. The possible origins of such inconsistency are beyond the scope of the current work. We limit ourselves here to recommending better sampling techniques for future FPMD studies of silicate melts in order to ensure that 1) the partition function at high temperature and high pressure is adequately sampled, 2) the thermo-physical properties obtained from these simulations reflect their true equilibrium behaviour, and 3) the functional form of the excess volume reflects a fundamental understanding of the link between internal energy, structure and volume.

The present work is organized as follows: the classical thermodynamic description of the thermo-physical behaviour of multicomponent liquid solutions is presented in section II. Approaches used to represent v^{xs} as a function of T, P and X are presented in section III. The thermodynamic model parameterization procedure for the MgO-SiO_2 liquid solution at P_0 is explained in section IV. Results of the parameterization of v^{xs} for the MgO-SiO_2 binary system using different approaches and the resulting derived thermo-physical excess properties are given in section V and section VI respectively. The predicted MgO-SiO_2 phase diagram in the SiO_2-rich region for different pressures is presented in section VII. We close with some perspectives in section VIII and conclusions in section IX.

II. Classical thermodynamic description of the thermo-physical properties of multicomponent liquid solutions

We summarize here (more detail is given in Appendix 1) the basis of a thermodynamic model for mixing in multicomponent liquid solutions that explicitly takes account of short-range atomic ordering and its extension to high pressure. Such a model requires definition of the Gibbs energy of mixing as a function of configuration and composition, a correct formulation of the configurational entropy, and a formulation of the excess volume. Together these enable determination of the configuration parameters by Gibbs energy minimization. We discuss each element in turn.

II-A *The modified quasichemical model in the second nearest neighbour approximation*

The modified quasichemical model in the second nearest neighbour approximation was presented in detail by Pelton and Blander (1986). For silicate melts, it involves the definition of a cation second nearest neighbour quasichemical reaction. For MgO-SiO_2, the following reaction is defined:

$$[\mathrm{Si}-\mathrm{Si}]+[\mathrm{Mg}-\mathrm{Mg}]\rightarrow 2[Mg-Si];\quad \Delta g^{QC}_{Si-Mg} \tag{1}$$

The variation of the molar Gibbs energy of the quasichemical model reaction Δg^{QC}_{Si-Mg} was originally expressed as a polynomial in the component equivalent fractions and temperature *T*:

$$\Delta g^{QC}_{Si-Mg} = \sum_{i+j\geq 0} \left(\omega_{ij} + \eta_{ij} T\right) Y^{i}_{SiO_2} Y^{j}_{MgO} \tag{2}$$

Pelton *et al.* (2000) later introduced excess parameters of this quasichemical reaction that can be a function of pair fractions. The general definition of Y_i, the equivalent pair fraction of species *i*, is:

$$Y_i = \frac{z_i \cdot X_i}{\sum_{j=1}^{s} z_j \cdot X_j} \tag{3}$$

where X_i is the molar fraction of the i^{th} species in the melt. An equivalent partial coordination number for each species, z_i, is introduced in the thermodynamic model to modify the position of the minimum in the molar Gibbs energy of mixing function as explained by Pelton and Blander (1986). The partial coordination numbers define the total coordination number of the solution $z_{tot.}$:

$$z_{tot.} = \sum_{i=1}^{s} z_i \cdot X_i \tag{4}$$

The number of moles of second nearest neighbour pairs *i-j*, n_{i-j}, is related to the number of moles of each system species via the following mass balance:

$$z_i \cdot n_i = 2n_{i-i} + \sum_{j\neq i}^{s} n_{i-j} \tag{5}$$

II-B *The configurational entropy of mixing*

In this work, the molar configurational entropy of mixing of the modified quasichemical model in the second nearest neighbour approximation, $\Delta s^{QC,config.}$, is used:

$$\Delta s^{QC,config.} = -R \cdot \left[\sum_{i=1}^{s} X_i \ln\left(X_i\right) + \frac{z_{tot.}}{2} \left[\sum_{i=1}^{s} X_{ii} \ln\left(\frac{X_{ii}}{Y_i^2}\right) + \sum_{j>i}^{s} \sum_{i=1}^{s} X_{ij} \ln\left(\frac{X_{ij}}{2 \cdot Y_i Y_j}\right) \right] \right] \quad (6)$$

This model (Pelton *et al.*, 2000) involves the introduction of second nearest neighbour pair fractions X_{ij}. Although more recent modifications have been made to this model (Pelton *et al.*, 2000) especially for the definition of $z_{tot.}$ as a function of the chemical composition, we decided to use this original model for comparison with previous similar thermodynamic assessments (Hudon *et al.*, 2004, 2005; Wu *et al.*, 1993). We emphasize the critical advantage of the quasichemical method, as compared to the regular solution or associated solution approach commonly adopted in geochemical solution modeling: that the explicit consideration of microscopic order in the quasichemical approach makes the configurational entropy internally consistent with the excess enthalpy of the solution.

II-C Total Gibbs energy of mixing at ambient pressure

With all the variables of this model properly presented, one can define the total Gibbs energy of mixing for the SiO_2-MgO binary system at ambient pressure:

$$\Delta G^{QC,mix.}\left(T, P_0, \underline{X}\right) = -T\left(n_{tot.} \cdot \Delta s^{QC,config.}\right) + \frac{n_{Si-Mg}}{2} \Delta g^{QC}_{Si-Mg} \quad (7)$$

where the chemical composition vector is defined as $\underline{X} = \left[X_1, X_2, ..., X_s\right]$. The total Gibbs energy of the solution is obtained by minimizing eq. 7 constrained by the mass balances presented previously. The equilibrium abundance of each pair is governed by eq. 7: a large and negative value for Δg^{QC}_{Si-Mg} will favor the presence of Mg-Si pairs in the melts at the expense of Mg-Mg and Si-Si pairs, while a large and positive value will favor unmixing, i.e. the formation of Mg-Mg and Si-Si pairs. If $\Delta g^{QC}_{Si-Mg} = 0$, no pairs are favored and the solution is said to be ideal. This thermodynamic model is therefore an implicit function of the pair fractions. If pressure

dependent terms are added to eq. 2 as proposed in the simplified approach of Robelin *et al.* (2007) to define density of molten salts, then the model is also an implicit function of pressure, as pair fractions will evolve as a function of this variable.

Finally, configuration-independent contributions that will not affect the magnitude of each pair fraction in the melt, also called Bragg-Williams-like excess parameters, can be added to eq. 7. Such excess terms, i.e. Margules parameters, are familiar from models more commonly used in geochemistry such as the regular and associated solution models. For the MgO-SiO_2 binary system, configuration-independent molar excess Gibbs energy $\Delta g^{BW,xs}$ takes the following general form:

$$\Delta g_{Si-Mg}^{BW,xs} = \frac{z_{tot.}}{2}\left[Y_{SiO_2} Y_{MgO} \sum_{i+j\geq 0} \left(\omega_{ij} + \eta_{ij} \cdot T\right) Y_{SiO_2}^{i} Y_{MgO}^{j} \right] \quad (8)$$

II-D ***The effect of pressure through the excess volume***

The energetic effects of pressure on silicate melts are based on the explicit definition of a function describing the change in molar excess Gibbs energy upon compression:

$$\Delta g_{P_0 \to P}^{xs}\left(T, P, \underline{X}\right) = \int_{P_o}^{P} v^{xs}\left(T, P, \underline{X}\right) dP \quad (9)$$

with:

$$v^{xs}\left(T, P, \underline{X}\right) = v^{solution}\left(T, P, \underline{X}\right) - \sum_{i=1}^{s} X_i \cdot v_i^0\left(T, P\right) \quad (10)$$

The function $\Delta g_{P_0 \to P}^{xs}\left(T, P, \underline{X}\right)$ defined in eq. 9 represents the molar Gibbs energy change associated with modifying the equilibrium state of the melt from a reference pressure P_0 (atmospheric pressure) to a final pressure P at a given T and composition. In eq. 10, $v^{solution}$ is the molar volume of the solution and v_i^0 represents the molar volume of each constitutive species i of the solution. As presented here, the analytical form of $v^{xs}\left(T, P, \underline{X}\right)$ and its resulting integrated expression with respect to pressure will depend on the thermodynamic model considered, as well as assumptions regarding its behaviour as a function of the internal structure of the solution. In

this case we considered that the excess volume goes to zero as a function of pressure. The complete definition of the total Gibbs energy of silicate melts using this approach is presented in Appendix 1.

II-E *Distinctions between configuration-dependent and configuration-independent excess parameters at P_0*

As stated previously, the quasichemical model in the second nearest neighbor pair approximation permits variation of the degree of Short Range Order (SRO) in the solution via variation of the molar Gibbs energy of the quasichemical reaction Δg^{QC}_{A-B}. It has been shown in our recent studies on metallic systems (Harvey *et al.*, 2011, 2012) that configuration-independent excess contributions could also be physically present in the solution, even if a certain degree of SRO is observed. For example, if volume relaxation effects occur in the NPT ensemble then excess terms will be needed to adequately represent the Gibbs energy of the solution, but this should not affect or depend on the speciation. As proposed by Pelton and Kang (2007), a combination of different configuration-dependent (quasichemical) and configuration-independent (Bragg-Williams) excess parameters can be used to model the system with a higher degree of accuracy.

In the case of the MgO-SiO_2 binary system at ambient pressure, the previous thermodynamic assessment using this model reported by Wu *et al.* (1993) considered only the presence of configuration-dependent excess terms. In this system, it is reasonable to assume that the maximum amount of SRO will occur at a molar composition of $X_{SiO_2} = 1/3$ where two Mg^{2+} cations and one Si^{4+} cation form an ionic complex Mg_2SiO_4. In the solid state, Mg_2SiO_4 is the most stable compound of the system (Fei *et al.*, 1990). A negative and configuration-dependent enthalpy term should be added to the thermodynamic model to represent this physical behaviour. According to Hudon and Baker (2002a, b), one explanation of the origin of the liquid miscibility gap observed in this liquid slag system is due to the difference in cation size between Si^{4+} and Mg^{2+}. Hence, the positive enthalpy contribution inducing the miscibility gap should reasonably be modelled using configuration-independent excess terms. New FPMD molar enthalpy of mixing data simulated at 0 GPa are also available and could modify the thermodynamic assessment of this system. For these reasons, we decided to perform a new thermodynamic assessment of the MgO-SiO_2 system at ambient pressure.

By analogy and as a direct consequence of these observations, it is important to explore the possibility of using configuration-independent and configuration-dependent excess volumes in this work.

III. Choices of excess volume expressions

If we suppose, for the moment, that the excess volume is configuration independent, then an analytical form for $\Delta g^{xs}_{P_0 \to P}\left(T,P,\underline{X}\right)$ can be obtained. Although we mentioned earlier that configuration-dependent parameters are permissible and might be expected in the parameterization procedure, the thermo-physical properties obtained from FPMD simulations by de Koker *et al.* (2013) do not in practice require such parameters.

III-A *Configuration-independent Bragg-Williams polynomial representation of the excess volume for low pressure*

For low pressures (a few GPa), one can assume that the molar excess volume can be expanded as a function of the species equivalent fractions, temperature and pressure according to the following power series:

$$v^{xs}\left(T,P,\underline{X}\right) = Y_1 Y_2 \sum_{i+j\geq 0}\left[\sum_{q\geq 0}\left[l_{ij}^{q} + k_{ij}^{q}\cdot T\right]\left(P-P_0\right)^{q}\right] Y_1^{i} Y_2^{j} \qquad (11)$$

Note that when $q=2$, eq. 11 is the excess function equivalent of the equation of state used by Ghiorso (2004a, b, c; Ghiorso and Kress, 2004) (if a and b are equal to 0). Derived excess thermodynamic properties of this formalism can be found in Appendix 2.

Because derived properties such as isothermal compressibility and volumetric thermal expansivity data can also be available for the solution, it is important to define the excess isothermal compressibility β_T^{xs} and the excess volumetric thermal expansivity α_V^{xs}:

$$\beta_T^{xs} \equiv -\frac{1}{v^{xs}}\left(\frac{\partial v^{xs}}{\partial P}\right)_T \qquad (12)$$

$$\alpha_V^{xs} \equiv \frac{1}{v^{xs}}\left(\frac{\partial v^{xs}}{\partial T}\right)_P \qquad (13)$$

These two excess physical properties are not extensive properties and thus cannot be evaluated from simple mixing rules. In order to define and use simple mixing rules, the following two extensive physical quantities are introduced:

$$\Gamma^{xs} \equiv \left(\frac{\partial v^{xs}}{\partial P} \right)_T = -v^{xs} \beta_T^{xs} \tag{14}$$

$$\Omega^{xs} \equiv \left(\frac{\partial v^{xs}}{\partial T} \right)_P = v^{xs} \alpha_v^{xs} \tag{15}$$

Γ^{xs} is the extensive excess isothermal compressibility of the solution, whereas Ω^{xs} is the extensive excess isobaric thermal expansion. These two derived extensive excess properties can be used to parameterize the expression defining the excess volume:

$$\Gamma^{xs}\left(T,P,\underline{X}\right) = \left(\frac{\partial v^{xs}}{\partial P} \right)_T = Y_1 Y_2 \sum_{i+j\geq 0} \left[\sum_{q\geq 1} q \cdot \left(l_{ij}^q + k_{ij}^q \cdot T \right) \left(P - P_0 \right)^{q-1} \right] Y_1^i Y_2^j \tag{16}$$

$$\Omega^{xs}\left(T,P,\underline{X}\right) = \left(\frac{\partial v^{xs}}{\partial T} \right)_P = Y_1 Y_2 \sum_{i+j\geq 0} \left[\sum_{q\geq 0} k_{ij}^q \left(P - P_0 \right)^q \right] Y_1^i Y_2^j \tag{17}$$

To allow the excess volume to vary as a function of both pressure and temperature, at least one l_{ij}^1 and one k_{ij}^0 parameter have to be assigned a non-zero value according to eqs. 16 and 17. Moreover, if β_T^{xs} varies as a function of pressure, then at least one l_{ij}^{2+n} parameter with $n \geq 0$ should be used.

These two physical quantities ultimately lead to the expression of β_T^{xs} and α_V^{xs} as a function of the pure species (Γ_i, Ω_i) and the solution physical properties ($\Gamma^{solution}, \Omega^{solution}$):

$$\beta_T^{xs} = -\left[\frac{\Gamma^{solution} - \sum_{i=1}^{s} x_i \Gamma_i}{v^{xs}} \right] \tag{18}$$

$$\alpha_V^{xs} = \frac{\Omega^{solution} - \sum_{i=1}^{s} x_i \Omega_i}{v^{xs}} \tag{19}$$

We will see that these two last equations can be used to judge the validity and coherence of the data.

III-B *Configuration-independent Bragg-Williams exponential decay representation of the excess volume for moderate-to-high pressure and high temperature*

For moderate-to-high pressure and temperature, the limiting behavior of v^{xs} is not clearly established in the literature. Proposing a functional form of v^{xs} under these extreme conditions becomes a difficult task. In order to reproduce the set of thermo-physical properties presented by de Koker *et al.* (2013), we are using here one of their important FPMD simulation observations, i.e. "*the volume of mixing becomes increasingly ideal at elevated pressure*. *Indeed* v^{xs} *is essentially zero over most of the lower mantle*". This assumption is consistent with, though not required by, shock wave experiments of Asimow and Ahrens (2010) on three compositions along a different multicomponent silicate liquid join, the $CaMgSi_2O_6$-$CaAl_2Si_2O_8$ binary. The volume of the intermediate composition, at high temperature along the Hugoniot, can be predicted from the end-member equations of state, whereas the excess volume inferred at low temperature is prone to high uncertainties (Asimow and Ahrens, 2010). Following de Koker *et al.* (2013), the limiting behaviour of v^{xs} at high pressure and temperature is assumed to be as follows:

$$\lim_{T\to\infty} v^{xs}\left(T,P,\underline{X}\right) = 0 \tag{20}$$

$$\lim_{P\to\infty} v^{xs}\left(T,P,\underline{X}\right) = 0 \tag{21}$$

According to eqs. 20 and 21, the excess volume becomes increasingly ideal for both elevated pressure and temperature. To respect eqs. 20 and 21 simultaneously, the following expression is proposed:

$$v^{xs}\left(T,P,\underline{X}\right) = Y_1 Y_2 \sum_{i+j\geq 0} \left[\left[a_{ij} + b_{ij}T + c_{ij}\left(P-P_0\right)\right] exp\left[d_{ij}\left(P-P_0\right) + f_{ij}T\right]\right] Y_1^i Y_2^j \tag{22}$$

Excess thermodynamic properties such as I^{xs} and Ω^{xs} (equivalent to eq. 16 and eq. 17) derived from this specific representation of v^{xs} are presented in Appendix 2. Important limitations of this functional form must be stated at this point. According to the calculated self-diffusivities of Si and Mg cations in MgO-rich silicate melts obtained by de Koker *et al.* (2008), the FPMD simulations of de Koker *et al.*(2013) are most probably not run long enough (6 ps) for two immiscible liquids to develop, even when the liquid lies inside the spinodal region. Indeed, a first indication that can be used to qualitatively assess the necessary time to relax silicate melt structures in MD simulations can be found in the work of Karki et al. (2013). These authors evaluated the viscosity of MgO-SiO_2 melts at ambient pressure. In their work, the authors present the evolution of the normalized stress auto-correlation function as a function of the MD simulation time. As the amount of SiO_2 increased, the relaxation time drastically increased, going up to the ns scale for pure SiO_2 liquid. A reasonable relaxation time at 3000 K and atmospheric pressure would be well above 30 ps for SiO_2-rich melt. However, this is not a sufficient criterion since any given configuration can be relaxed. In order to 1) reach the equilibrium state and 2) simulate enough configurations to sample adequately the partition function, much longer simulation times would be required. In this case, self-diffusion coefficient could be used to qualitatively assess the suitable relaxation/equilibration time for each composition. This topic has been covered in the recent work of Harvey and Asimow (2015).

Obviously, eq. 22 applies to single-phase regions only, though in some cases that single liquid may be metastable or unstable. We will see in section VIII how the miscibility gap calculated from this formulation compares to the available experimental data for the MgO-SiO_2 system (Dalton and Presnall, 1997; Hudon *et al.*, 2004, 2005). The high-pressure limiting behaviour of equation (22) is not based on fundamental physical concepts or experimental observations; it is motivated by the interpretation of de Koker *et al.* (2013) and therefore should allow a self-consistent thermo-physical interpolation of the FPMD data. The assumption of the temperature limiting behaviour of v^{xs}, eq. 22, on the other hand, is believed to be reasonable, because any system at high temperature will tend towards the ideal gas limit.

III-C. Configuration-dependent quasichemical-like excess volume formulations

As presented in section II, the thermodynamic behaviour of liquid silicate melts can be expressed, in part, as a function of second nearest neighbour pair fractions X_{ij}. Eqs. 11 and 22

describing v^{xs} might thus, in principle, be re-written as a function of these variables. In this work, we did not explore this option because the FPMD simulations show that the largest excess volume phenomena are present on the SiO_2-rich side of the system where configuration-independent contributions are dominant. However, for completeness we note that in situations where excess volume does need to be written in terms of configuration-dependent pair fractions, a problem arises from the pressure and temperature dependencies of the X_{ij}. No analytical form for $\Delta g^{xs}_{P_0 \to P}\left(T, P, \underline{X}\right)$ can be obtained in this case. To partially circumvent this problem one can change the order of evaluation, beginning from a general form for $\Delta g_{AB}\left(T, P, X_{ij}\right)$, and numerically evaluating all thermo-physical properties from Gibbs energy minimization.

IV. Thermodynamic model parameterization procedure of the MgO-SiO_2 liquid solution at P_0

The classical scheme for the parameterization of the selected thermodynamic model, in this case the modified quasi-chemical model in the second nearest neighbour formalism (Pelton and Blander, 1986), is found extensively in the literature. A new approach that considers simultaneously both thermodynamic and structural self-consistent data was presented recently in the case of metallic systems (Harvey *et al.*, 2011, 2012). To apply this self-consistent approach, enthalpy, entropy, and structural data at P_0 for each potentially stable solution have to be evaluated in order to completely represent their respective thermo-physical behaviour. Phase diagram data are used in this case to validate the parameterization or to fine-tune the excess properties of the solution. One has to remember that multi-phase equilibria are defined by common tangents and that, accordingly, a small local shift in the Gibbs energy of a given solution could potentially drastically affect the phase assemblage.

The recent FPMD study of de Koker *et al.* (2013) provides the most complete set of self-consistent thermo-physical data as a function of T, P and X for any multi-component silicate liquid, in this case the MgO-SiO_2 binary. However, de Koker *et al.* (2013) did not have access to a direct method for evaluating the mixing entropy at P_0 and did not present partial distribution functions needed to evaluate structural data such as second nearest neighbour pair fractions. Therefore we performed a classical thermodynamic parameterization at P_0 to accurately obtain the Gibbs energy function of the liquid solution at this pressure. Other thermodynamic

assessments for this system were proposed by Wu *et al.* (1993), Holland and Powell (2003) and Ghiorso *et al.* (2002).

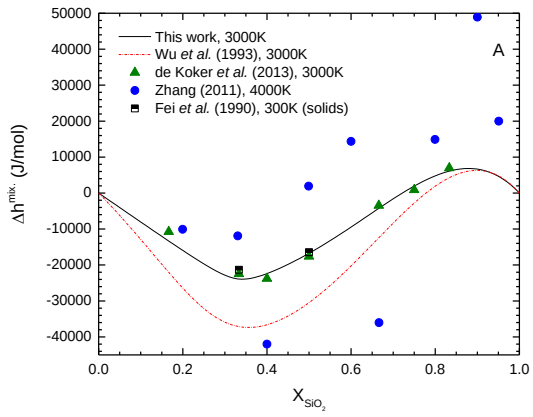

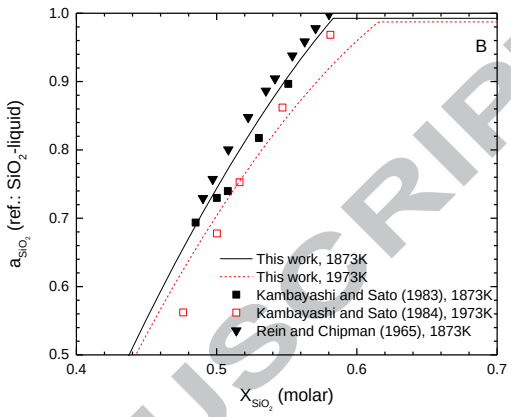

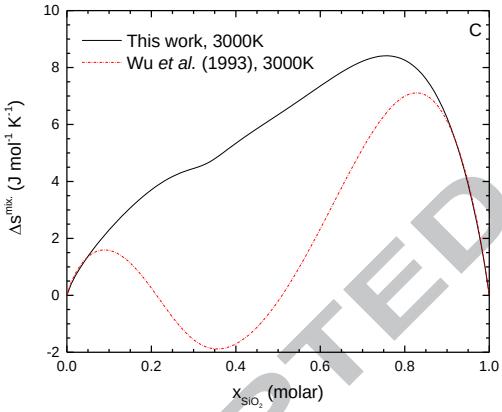

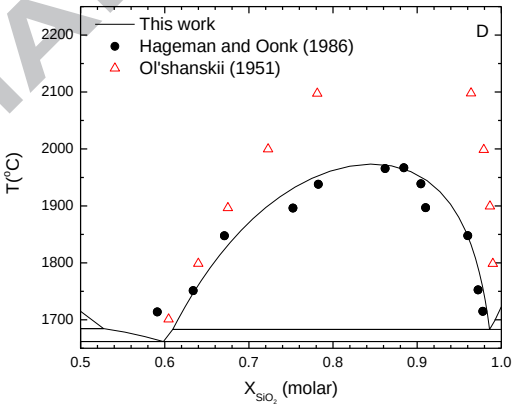

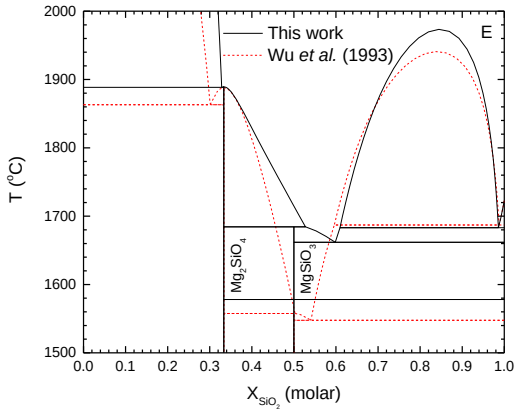

Figure 1: Results of the CALPHAD method thermodynamic assessment of the MgO-SiO_2 liquid phase at 0 GPa: A) molar enthalpy of mixing; B) SiO_2-liquid activity data (note, this plot continues into the stability fields of Mg_2SiO_4 and $MgSiO_3$; the metastable liquid is plotted for illustration purposes); C) molar entropy of mixing; D) liquid-liquid miscibility gap; and E) Entire phase diagram.

Table 1: Thermodynamic parameters of the MgO-SiO_2 liquid solution obtained for P_0

Excess parameter	Numerical value
Z_{Mg}	1.3774
Z_{Si}	2.7548
Δg^{QC}_{Si-Mg}	
ω^{QC}_{00}	-58576 J·mol^{-1}
η^{QC}_{00}	-17.99 J·mol^{-1}·K^{-1}
$\Delta g^{BW,xs}_{Si-Mg}$	
η^{BW}_{00}	23.43 J·mol^{-1}·K^{-1}
ω^{BW}_{70}	239325 J·mol^{-1}
η^{BW}_{70}	-86.19 J·mol^{-1}·K^{-1}

We performed a CALPHAD method thermodynamic assessment of the liquid phase using FactSage software (Bale *et al.*, 2009), with an emphasis on accurately fitting the FPMD molar heat of mixing data of de Koker *et al.* (2013). In our approach, the thermodynamic description of each solid phase and of pure MgO(liq.) and SiO_2(liq.) is taken directly from the work of Wu *et al.* (1993). The resulting properties and optimized phase diagrams are shown in Figure 1 and the thermodynamic parameters of the quasichemical model are presented in Table 1.

FPMD enthalpy of mixing data obtained by Zhang (2011) at 4000 K are also shown in Fig. 1A. These results highlight the potentially large uncertainty in evaluating thermodynamic properties with this technique. Zhang (2011) attributed this large uncertainty to several factors. MD simulations are sensitive to initial configuration; integration of the equations of motion identifies only local minima and samples a limited part of the Gibbs energy surface of the solution. Zhang (2011) used three initial configurations. The resulting standard deviation of the total energy is between 10 and 50 kJ/mol, which could induce a potentially large absolute error in calculating molar heat of mixing. It is unclear whether such errors are present in the results of de Koker *et al.* (2013), who begin each simulation only from a single initial configuration. Moreover, the total simulation time directly impacts the statistical analysis required to evaluate thermodynamic properties of the system. This statistical analysis is also used to ensure that the simulations are ergodic. Short simulation times, given the low self-diffusivity of Si at some of the state points and compositions studied, limits the number of chemical configurations sampled by MD simulations. The simulations of de Koker *et al.* (2013) and of Zhang (2011) used similar simulation times (6ps) and number of atoms (≈100), suggesting that the apparently better internal precision and lower reported uncertainties de Koker *et al.* (2013) may result from the use of only one initial configuration for each state point; it is difficult to tell from the published record.

Wasserman *et al.* (1993) reported a maximum in the enthalpy of mixing of MgO-SiO_2 melts of +22 kJ/mol at $X_{SiO_2} = 0.7$, obtained by classical MD simulations at 5000 K and 5 GPa with an accuracy of 10 kJ/mol, while predicting all negative values at 50 GPa. As a basis of comparison, the calculated molar enthalpy of mixing obtained by Wu *et al.* (1993) in their thermodynamic assessment of the MgO-SiO_2 system is presented in Fig 1A.

Entropy parameters of the quasichemical model for the liquid phase presented in Table 1 are obtained by fitting experimental activity data reported by Kambayashi and Kato (1983, 1984) and of Rein and Chipman (1965) (Fig. 1B) as well as the liquid-liquid miscibility gap data of Hageman and Oonk (1986) in the SiO_2-rich side of the phase diagram (Fig. 1D). FPMD alone cannot provide the absolute entropy of a given equilibrium state unless an approach such as the thermodynamic integration method is implemented to overcome this limitation. It is therefore of fundamental importance to use all these thermodynamic data to fine-tune the entropy of the solution. A comparison between the predicted molar entropy of mixing obtained in this work and by Wu *et al.* (1993) is presented in Fig. 1C. Finally, the entire liquidus of the MgO-SiO_2 system obtained from the present thermodynamic assessment is compared to that of Wu *et al.* (1993) in Fig. 1E. We did not use the temperatures and compositions of the eutectic and peritectic points as constraints because this makes the liquid model strongly dependent on the adopted solid models; hence the detailed liquidus topology in the middle of the diagram is a prediction or confirmation of our model rather than a fit forced by the calibration. There is a discrepancy in the liquidus between the two assessments, up to 150°C, between X_{SiO_2} = 0.4 and X_{SiO_2} = 0.6. This error is caused by a change of about 2 kJ/mol in the Gibbs energy of the liquid phase, which is relatively small compared to typical errors of FPMD simulations. In general phase diagram topologies are sensitive to differences in Gibbs energy below the resolution of FPMD simulations and the accurate prediction of phase equilibria data requires additional tuning such as the incorporation of univariant temperatures and compositions as constraints.

V. Parameterization procedure of $\Delta g^{xs}_{P_0 \to P}(T, P, \underline{X})$

To calculate the effect of pressure on the Gibbs energy function calibrated at P_o in section IV, we attempt to parameterize $\Delta g^{xs}_{P_0 \to P}(T, P, \underline{X})$ using both eq. 11 and eq. 22.

Note that all the equations of section III and corresponding Appendixes must be multiplied by a coordination number factor $z_{tot}./2$ to conform with the quasichemical formalism implemented in the *FactSage* software. The numerator of this coordination number factor is the equivalent coordination number of the solution (eq. 4), while the denominator is the coordination number of the classical quasichemical model ($z_{classical}$ = *2*). For a given set of excess parameters in eqs. 11

and 22, $\Delta g^{xs}_{P_0\to P}\left(T,P,\underline{X}\right)$ scales by the equivalent coordination number of the solution according to this formalism, so all thermodynamic properties presented in section III are normalized by this factor.

Figs. 2A and 2B present the results of the least squares fitting of FPMD molar volume and enthalpy of mixing data at 3000 K and each pressure reported by de Koker *et al.* (2013) to the following functions:

$$\left(\frac{v^{xs}\left(\underline{X}\right)}{z_{tot.}/2}\right)_{T,P} = Y_{SiO_2}Y_{MgO}\left[\left(\beta_{00}\right)_{T,P}+\left(\beta_{70}\right)_{T,P}Y^{7}_{SiO_2}\right] \tag{24}$$

$$\left(\frac{\Delta h^{xs}_{P_0\to P}\left(\underline{X}\right)}{Z_{tot.}/2}\right)_{T,P} = \left(\frac{h^{xs}_{P}\left(\underline{X}\right)-h^{xs}_{P_0}\left(\underline{X}\right)}{Z_{tot.}/2}\right)_{T,P} = Y_{SiO_2}Y_{MgO}\left[\left(\omega_{00}\right)_{T,P}+\left(\omega_{70}\right)_{T,P}Y^{7}_{SiO_2}\right] \tag{25}$$

The general form of these equations is similar to the BW excess parameter function used in section IV to fit the thermo-physical properties at P_0. The same powers (0^{th} and 7^{th}) were adopted for the excess configuration-independent parameters at P_0 and allowed description of the miscibility gap in the silica-rich region. Note that open symbols in Fig. 2B are apparently anomalous FPMD data of de Koker *et al.* (2013) that were excluded from the least squares fitting procedure.

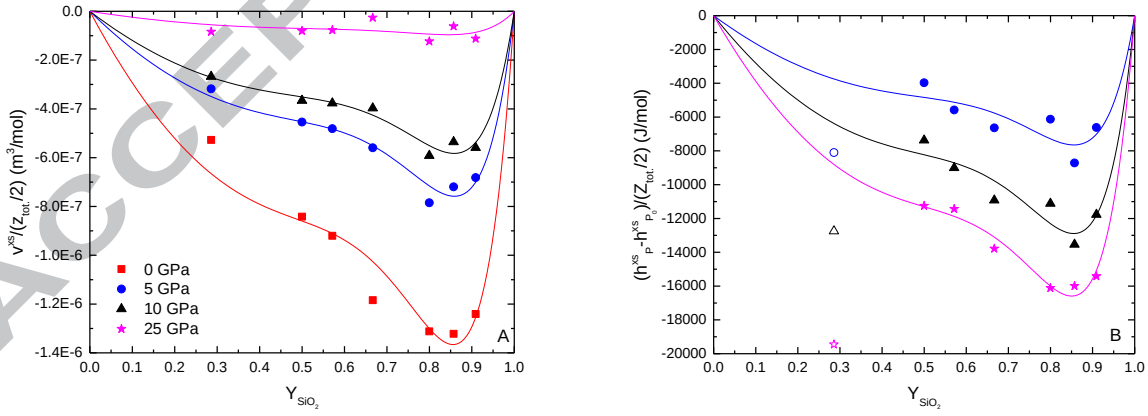

Figure 2: Results of the least squares fitting of A) $\left(\frac{v^{xs}}{z_{tot.}/2}\right)$ and B) $\left(\frac{h_P^{xs}-h_{P_0}^{xs}}{z_{tot.}/2}\right)$ as a function of Y_{SiO_2} at each pressure. Symbols represent the FPMD data of de Koker *et al.* (2013), while solid lines are functions fitted in this work. Open symbols in B) are FPMD data of de Koker *et al.* (2013) that are not considered in the least squares fitting procedure.

The fitted parameters defining $\left(\frac{v^{xs}}{z_{tot.}/2}\right)$ and $\left(\frac{h_P^{xs}-h_{P_0}^{xs}}{z_{tot.}/2}\right)$ using eqs. 24 and 25 at each pressure are summarized in Figs. A-1 and A-2 (Appendix 3). The observation that v^{xs} tends to zero as pressure increases, made by de Koker *et al.* (2013), is consistent with these results, with the excess volume parameters (Fig. A-1) tending to zero and the excess enthalpy parameters (Fig. A-2) converging to constants at high pressure. These observations motivate the general form of eq. 22 for moderate-to-high pressures (section III-B).

V-A *Low pressure polynomial representation of v^{xs} (below 10 GPa)*

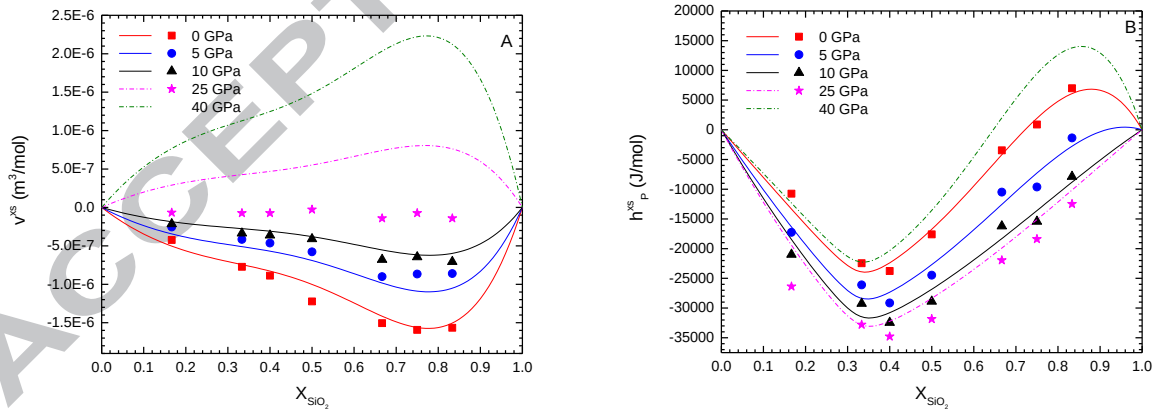

Figure 3: Results of the parameterization of eqs. 11 and A2-3 that allows the description of A) v^{xs} and B) h_P^{xs} as a function of X_{SiO_2} and P. Symbols in this figure are the FPMD data of de Koker *et al.* (2013) while the lines are the results obtained from eqs. 11 and A2-3.

At low pressure, i.e. below 10 GPa, we assume that the parameters of both $\left(\frac{v^{xs}}{z_{tot.}/2}\right)$ and $\left(\frac{h_P^{xs}-h_{P_0}^{xs}}{z_{tot.}/2}\right)$ are linear functions of pressure, i.e. $q=1$ in eq. 11 (Figs. A-1 and A-2 in Appendix 3 make it clear that this assumption does not apply over larger pressure ranges). As mentioned previously, this is the minimum requirement for defining Γ. Also, both enthalpy $\left(l_{ij}^{q}\right)$ and entropy $\left(k_{ij}^{q}\right)$ parameters are used in order to fit simultaneously these two thermodynamic properties as a function of pressure and to define Ω. Enthalpy parameters are obtained first by fitting molar heat of mixing data (see eq. A2-3). Molar volume data are then used to parameterize the entropy terms. Optimized parameters for eq. 11 using this procedure are presented in Table 2.

Table 2: Optimized parameters of eq. 11 defining $\left(\frac{v^{xs}}{z_{tot.}/2}\right)$

Parameter	Value
l_{00}^{0}	-4.214E-06 J/(mol·Pa)
l_{70}^{0}	-3.014E-05 J/(mol·Pa)
l_{00}^{1}	2.184E-16 J/(mol·Pa^2)
l_{70}^{1}	1.672E-15 J/(mol·Pa^2)
k_{00}^{0}	3.823E-10 J/(mol·K·Pa)
k_{70}^{0}	2.674E-09 J/(mol·K·Pa)
k_{00}^{1}	-8.265E-21 J/(mol·K·Pa^2)

k_{70}^{1}	-1.185E-19 J/(mol·K·Pa^2)

V.B *Moderate pressure exponential decay representation of v^{xs} (at 10-25 GPa)*

For moderate pressures, eq. A2-6 is used to describe the FPMD data obtained by de Koker *et al.* (2013); fit parameters are given in Table 3. In this formalism, v^{xs} tends to zero as pressure goes to infinity. In fact, v^{xs} is almost 0 at about 40 GPa (Fig. 4A). The FPMD data do not cover enough temperatures to constrain the limiting behavior of v^{xs} as a function of temperature, so no f_{ij} parameters are used in this work. Using this formalism, it is possible to fit all raw thermo-dynamic data of de Koker *et al.* (2013) at 3000K with fairly good precision.

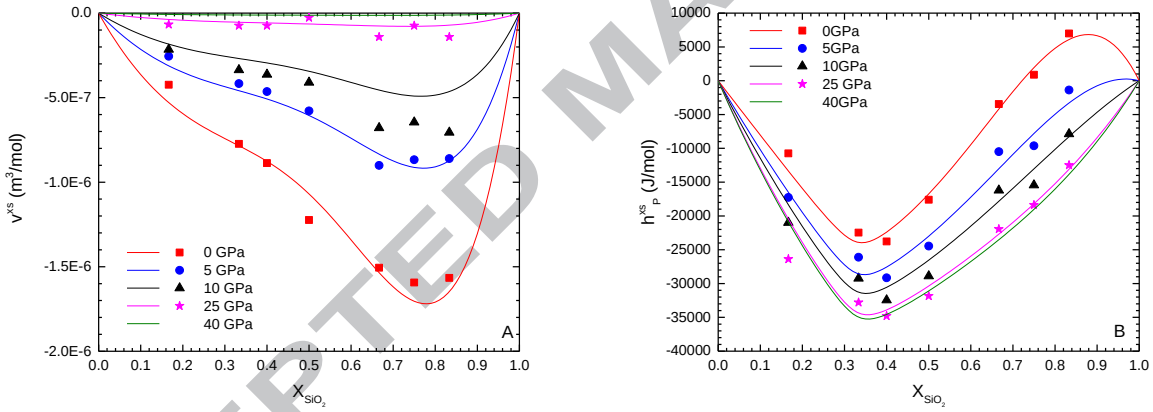

Figure 4: Results of the parameterization of eqs. 22 and A2-6 that allows the description of A) v^{xs} and B) h_P^{xs} as a function of X_{SiO_2} and P. Symbols in this figure are the FPMD data of de Koker *et al.* (2013) while the lines are the results obtained from eqs. 22 and A2-6.

Table 3: Optimized parameters of eq. 22 defining $\left(\frac{v^{xs}}{z_{tot.}/2}\right)$

Parameter	Value
a_{00}	-4.933E-06 J/(mol·Pa)
a_{70}	-3.777E-05 J/(mol·Pa)
b_{00}	5.693E-10 J/(mol·K·Pa)
b_{70}	4.429E-09 J/(mol·K·Pa)
c_{00}	--
c_{70}	--
d_{00}	-1.059E-10 (Pa^{-1})
d_{70}	-1.328E-10 (Pa^{-1})

VI. Calculation of derived thermo-physical excess properties

The proposed v^{xs} parameterizations enable calculation of derived excess properties such as Γ^{xs} and Ω^{xs} (defined in section III). Comparisons between the predicted behaviour of these two derived excess properties at 0 GPa and 3000 K using the polynomial representation of v^{xs} (valid for low pressure) and the data reported by de Koker *et al.* (2013) are presented in Figs. 5 and 6.

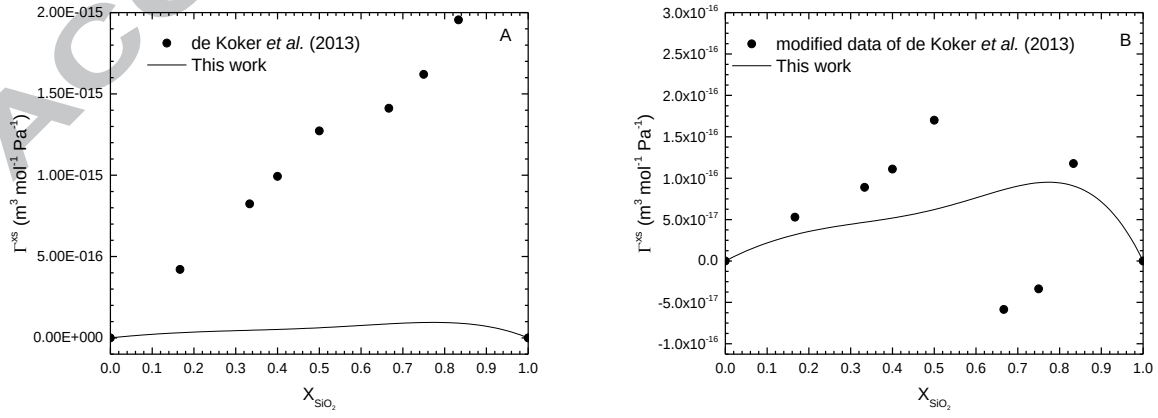

Figure 5: A) Γ^{xs} as a function of X_{SiO_2} for the MgO-SiO_2 melts at 0 GPa and 3000 K. Filled circles represent the data reported by de Koker *et al.* (2013); the solid line represents the results obtained in this work using the polynomial representation of v^{xs}, eq. 11. B) Magnification of the region showing the results obtained in this work (solid line). Filled circles now represent the data reported by de Koker *et al.* (2013) modified by referencing Γ^{xs} with respect to SiO_2 (liquid) having an isothermal bulk modulus of 12.2 GPa as proposed by de Koker and Stixrude (2009) for a 1st order expansion in θ.

These figures reveal important considerations when estimating derived excess properties from molecular dynamic simulations and parameterized Equations of State (EOS) for each studied composition. The first observation is the noticeable difference between Γ^{xs} obtained in this work compared to the data obtained by de Koker *et al.* (2013) using a 2nd-order expansion in dimensionless temperature (θ). This is a surprising result, since v^{xs} is well fitted in the low-pressure range using our approach (Fig. 3). However, de Koker and Stixrude (2009) demonstrate the effect of the order of the finite strain expansion on the resulting thermo-physical properties at 0 GPa for liquid SiO_2. The isothermal bulk modulus and its pressure derivative are highly sensitive to the order of the polynomial expansion in θ. The isothermal bulk modulus of 12.2 GPa that results from the 1st order expansion in θ would generate a set of Γ^{xs} values of amplitude much closer to our result (Fig. 5B). This is an important conclusion: the necessity of using a higher order finite strain expansion informs us that the behavior in temperature of liquid SiO_2 is of a complex form compared to MgO, Mg_2SiO_4 and $MgSiO_3$. It is critical in a future study to analyse carefully the low temperature FPMD simulations of liquid SiO_2 to see whether this complex behavior is reproducible or is instead a convergence issue with FPMD simulations of highly viscous melts at high pressure and low temperature.

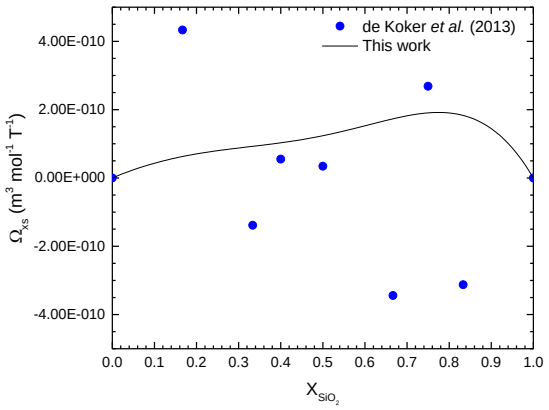

Figure 6: Ω^{xs} as a function of X_{SiO_2} for the MgO-SiO_2 melts at 0 GPa and 3000 K. Filled circles represent the data reported by de Koker *et al.* (2013); the solid line represents the results obtained in this work using the polynomial representation of v^{xs} (eq. 11).

The second observation is related to the precision of the calculation of Ω^{xs}. According to our work, Ω^{xs} calculated at 0 GPa and 3000 K is always positive and displays a smooth general behaviour similar to the other self-consistent excess properties. On the other hand, the Ω^{xs} data of de Koker *et al.* (2013) are scattered and of both signs. This may result from the indirect calculation procedure of the volumetric thermal expansion, α_V, which was not directly determined by de Koker *et al.* (2013) from the dependence of v^{xs} on T at P=0 GPa. Instead, the authors used the following thermodynamic identities,

$$\frac{1}{\beta_T} = V\left(\frac{\partial^2 F}{\partial V^2}\right)_T \qquad (26a)$$

$$\frac{\alpha_V}{\beta_T} = -\left(\frac{\partial^2 F}{\partial V \partial T}\right) \qquad (26b)$$

where F is the Helmholtz energy, in order to evaluate α_V from their parameterized EOS at each composition. This procedure is strictly equivalent to evaluating α_V from the macroscopic Grüneisen parameter γ:

$$\alpha_V = \frac{\gamma \cdot c_V \cdot \beta_T}{V} \tag{27}$$

where c_V is the molar heat capacity at constant volume. The error transfer from each thermo-physical property in eq. 27 is an important contribution to the scatter of the data seen in Fig. 6.

Moreover, Ω^{xs} values obtained from the FPMD data of de Koker *et al.* (2013), although scattered, seem to be distributed in two distinct regions: mostly positive deviations from ideality in MgO-rich melts and mostly negative deviations from ideality in SiO_2-rich melts. The uncertainty in locating these two regions and the definition of Ω^{xs} suggest a new thermodynamic criterion relating the sign of v^{xs} and Ω^{xs}. In section III-B, we mentioned that the v^{xs} function should converge to zero as the temperature increases without limit. In the case of uniformly negative excess volumes at 0 GPa (as reported by de Koker *et al.* (2013) for the MgO-SiO_2 system), a uniformly positive Ω^{xs} function (i.e. $\left(\frac{\partial v^{xs}}{\partial T}\right)_P > 0$) is necessary to reach the limit defined by eq. 20. On the other hand, a negative Ω^{xs} function should be expected alongside positive excess volumes at 0 GPa and finite temperature. Of course, violations of this principle over limited temperature ranges are possible, but require in turn even stronger converging behaviour beyond the studied range.

We do not propose a similar criterion for Γ^{xs} because the validity of eq. 21 is not based on fundamental physical principles. Moreover, it will be shown in section VII that this hypothesis is not valid and, most importantly, is inconsistent with the experimental phase diagram at low-to-moderate pressures for the MgO-SiO_2 system.

VII. Predicted evolution of $MgO\text{-}SiO_2$ miscibility gap

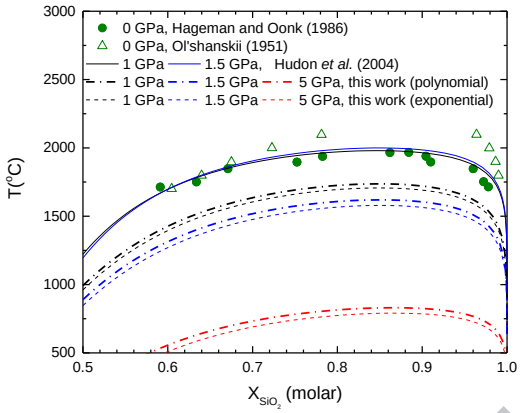

Figure 7: The liquid-liquid miscibility gap in the $MgO\text{-}SiO_2$ binary system as a function of pressure. The experimental data at 0 GPa of Ol'Shanskii (1951), Hageman and Oonk (1986) and of Hudon *et al.* (2004) for 1 GPa and 1.5 GPa are compared to the miscibility gaps predicted in this work using the polynomial (dashed and dot lines) and exponential decay (dashed lines) representations. This is not an equilibrium phase diagram; solid phases are suppressed to emphasize relations within the (possibly metastable) liquid phase only.

A decisive test for judging whether fitting the FPMD data of de Koker *et al.* (2013) with the v^{xs} equations proposed in this work captures the excess properties of the liquid solution is to predict the $MgO\text{-}SiO_2$ solvus on the SiO_2-rich side. In this region there is a miscibility gap at low pressure. The predicted $MgO\text{-}SiO_2$ miscibility gaps at each pressure obtained using the polynomial representation (eq. 11) and the exponential representation (eq. 22) are compared to the thermodynamic data given by Hudon *et al.* (2004) based on their experimental results (Fig. 7). In this figure, all solid phases are suppressed and only phase equilibrium data associated with the miscibility gap are considered. The prediction that results from our excess volume paramerization based on the FPMD data is a strongly decreasing consolute temperature from 0 to 5 GPa. According to the thermodynamic assessment of Hudon *et al.* (2004), however, the consolute temperature of the miscibility gap increases gently with pressure. This result awaits confirmation from experiments over a wider pressure range: in Fig. 7, consolute temperatures

between 1 and 1.5 GPa are well within the scatter of the 0 GPa experiments. Nevertheless, our prediction of decreasing consolute point behaviour with increasing pressure is inconsistent with that of Hudon *et al.* (2004).

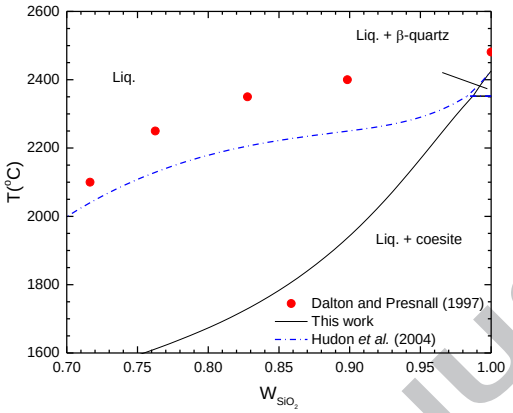

Figure 8: The silica liquidus in the MgO-SiO_2 binary at 5 GPa as a function of the weight fraction of SiO_2. Filled circles represent the data of Dalton and Presnall (1997); lines are the predicted liquidus obtained from the parameterization of the liquid phase in this work (solid line) and from Hudon *et al.* (2004) (dashed line).

It might be argued however that the most accurate set of data at 0 GPa is provided by Ol'shanskii (1951), contrary to what was claimed previously by Wu *et al.* (1993), in which case a decrease of consolute temperature with pressure, consistent with our model, would in fact reproduce the data of Hudon *et al.* (2005). But there is a further experimental constraint on the change in position of the solvus to be obtained by considering the silica liquidus data of Dalton and Presnall (1997) at 5.0 GPa (Fig. 8). According to these data, the liquid-liquid miscibility gap disappears by 5.0 GPa because of the significant increase of the melting point of SiO_2 with pressure (Hudon *et al.*, 2002) (proposed by Hudon *et al.* (1994)). The disappearance of the miscibility gap thus does not require a decrease of the consolute temperature. In fact the relatively flat shape of the experimental liquidus is a clear indication of a still-strong tendency toward demixing and suggests that the miscibility gap is not far below the liquidus at 5 GPa and therefore lies at higher temperature than the 1 bar consolute point. Although the shape of the liquidus depends only of

liquid-phase mixing properties, the absolute position of the calculated liquidus is sensitive to the Gibbs energy of the coexisting silica phase (in this case coesite). We chose the thermodynamic assessment of Hudon *et al*. (2002) to define the Gibbs energy function of coesite, but the uncertainty in the coesite liquidus is small enough that the conclusion that a strongly flattened liquidus at 5 GPa implies an increase in metastable consolute temperature is probably robust.

If the consolute temperature does in fact increase with pressure, then it is possible that the miscibility gap could reappear at higher pressures, where the rate of increase in liquidus temperature is much lower. Ultimately, the stable (not metastable) reappearance of a miscibility gap will be confirmed by performing equilibrium calculations that also account for the potential presence of the relevant SiO2 polymorphs for these particular equilibrium conditions. To achieve this objective, an accurate representation of the P-T unary phase diagram of SiO2 up to potentially very high pressure (50-100 GPa) is necessary and represent by itself a scientific challenge in geochemistry.

The disagreement at present between experimental observations and the self-consistent prediction calibrated upon first principles calculations, however, suggests that it is premature at this time to assess the very high-pressure behaviour of the miscibility gap. Further tests and independent calculations are needed to trace the source of the discrepancy to the experiments, to the interpolation method proposed here, or to the inherent accuracy of current FPMD simulations as a probe of mixing relations among SiO_2-rich liquids.

XIII. Discussion

Despite careful study, the evolution of the liquid-liquid miscibility gap in the MgO-SiO_2 binary system at high pressure is still not consistently accounted for. The shape of the experimental liquidus obtained by Dalton and Presnall (1997) at 5 GPa implies that the consolute point remains close to the liquidus and a potential reappearance of the miscibility gap at higher pressures is not impossible. It may be that the magnitude of the positive enthalpy of mixing in the liquid increases as a function of pressure, contrary to result derived from our self-consistent fit to the FPMD data of de Koker *et al.* (2013). In this scenario, the use of metastable single-phase simulation results at state points where the true equilibrium is a two-phase existence might bias the estimates of enthalpy of mixing. For instance, the FPMD heat of mixing data reported by

de Koker *et al.* (2013) at 0 GPa and 2000 K show that it would be energetically more favorable to form two immiscible liquids at $0.4 \leq X_{SiO_2} \leq 1$. The failure of the calculations to exsolve shows the need for caution in applying this method to potentially immiscible solutions, even though the entropic effects of mixing, which do not influence the equations of motion in molecular dynamics, might favour single-phase mixing by a Gibbs energy criterion.

Furthermore, Zhang (2011) showed that FPMD results are highly sensitive to initial configurations. Assuming that de Koker *et al.* (2013) started their simulations with a single-phase liquid solution, the energetic driving force inducing the formation of the miscibility gap at low pressure could have been insufficient. It is also possible that de Koker *et al.* (2013) reported thermodynamic properties of a two-phase liquid-liquid system. Where a miscibility gap is suspected it is important to analyze Si-Si, Si-Mg and Mg-Mg partial radial distribution functions and their change with pressure to detect incipient or complete exsolution.

Unfortunately, the existing literature on both classical and *ab initio* molecular dynamics of multicomponent silicate melts cannot resolve the origin of the inconsistency highlighted here. MD simulations of pure pseudo-unary liquids such as MgO (Alfè, 2005; Belonoshko and Dubrovinsky, 1996a; Karki *et al.*, 2006; Lacks *et al.*, 2007; Liu *et al.*, 2004) or SiO_2 (Benoit *et al.*, 2000; Carre *et al.*, 2008; Demiralp *et al.*, 1999; Feuston and Garofalini, 1988; Hassanali and Singer, 2007; Herzbach *et al.*, 2005; Karki *et al.*, 2007; Mitra *et al.*, 1981; Paramore *et al.*, 2008; Soules, 1990; Soules *et al.*, 2011; Takada *et al.*, 2004; Tangney and Scandolo, 2002; Tsuneyuki *et al.*, 1988; Vashishta *et al.*, 1990; Woodcock *et al.*, 1976) cannot provide any evidence regarding the importance of second-nearest neighbour SRO or its effect on thermo-physical properties at conditions relevant to Earth's mantle. Moreover, previous classical MD simulations of MgO-SiO_2 melts (Belonoshko and Dubrovinsky, 1996a; Ben Martin *et al.*, 2009; Oganov *et al.*, 2000; Spera *et al.*, 2011) did not explore the entire range of composition and do not address the present issue. Other classical MD simulations have been performed on geologically relevant multicomponent compositions (Ben Martin *et al.*, 2012; Guillot and Sator, 2007; Matsui *et al.*, 2000; Spera *et al.*, 2009) but in each case these studies examined only the thermo-physical properties of specific melt compositions and not excess properties of the solutions.

As the quasichemical model is unfamiliar to most geochemists, it will be interesting in the future to compare in greater detail the microscopic consequences of quasichemical solution models to those of the more familiar associated solution approaches. As an example, there is clearly a relationship in a statistical sense between the Si-Si pair fraction abundance of the quasichemical model, on the one hand, and the populations of "Q-species" (i.e. the number of Si-O-Si bridging oxygens coordinating each Si atom) considered by associated solution models (Hovis et al., 2004). Furthermore, the extent to which the points of minimum configurational entropy arising in a quasichemical model correspond to the precisely ordered compositions that result from assumed changes in the mixing species of an associated model, will clearly depend on the amplitude of the excess enthalpy of solution. For a value as negative as that optimized by Wu et al. for MgO-SiO_2 (-37.3 kJ/mol), the quasichemical approach will more nearly yield a perfectly ordered solution at the Mg_2SiO_4 composition that it would for the less negative enthalpy minimum given by the de Koker et al. simulation (-24.0 kJ/mol).

IX. Conclusion and perspectives

We present a new fully self-consistent approach to parameterizing the Gibbs energy of a multicomponent solution as a function of temperature, pressure and composition, using two representations of the excess volume. A well-constrained optimization following the usual CALPHAD practice for enthalpy and entropy of mixing at ambient pressure is obtained using FPMD data or activity-composition measurements and solid-liquid or two-liquid phase equilibrium constraints. Then the simultaneous least squares fit of molar volume and enthalpy of mixing data from FPMD simulations over a range of pressure results in the complete parameterization of the effect of pressure on the excess Gibbs energy of mixing, $\Delta g^{xs}_{P_0 \to P}\left(T, P, \underline{X}\right)$. We tested the utility of this approach for multicomponent silicate liquids of interest in geological science using using the published FPMD simulations data of de Koker *et al.* (2013) for the MgO-SiO_2 system. This exercise leads to several conclusions:

1. In the 0-25 GPa pressure range, a marked decrease with increasing pressure of the consolute temperature of the miscibility gap in the SiO_2-rich part of the system is predicted. This appears to be inconsistent with the phase equilibrium data. An increase in

the consolute temperature is more consistent with the 5.0 GPa liquidus data of Dalton and Presnall (1997).

2. Derived properties, such as the excess components of volumetric thermal expansion and isothermal compressibility, that are functions of composition and pressures are more accurately described using a consistent approach, as opposed to stitching together distinct equations of state fitted to each studied composition.
3. Thermodynamic inconsistencies between directly measured properties such as v^{xs} and derived excess thermo-physical properties via a given EOS (e.g., finite strain expansion), are easily detected with our approach.
4. A new thermodynamic criterion relating the sign of v^{xs} and its temperature dependence Ω^{xs}, based on the expected high temperature ideal limit, is proposed in section VI and should be tested in the future.

It may be assumed that the FPMD simulations of de Koker *et al.* (2013) have been performed with state-of-the-art methodology. Hence the evidence of discrepancies between predictions based on those simulations and experimental data urge caution concerning the accuracy of the Gibbs energy function derived from thermo-physical properties of liquids computed by FPMD simulations. In any particular case, a discrepancy could of course also be due to inconsistent experimental results used in the optimization. Comparable studies of more systems with independent experimental inputs are needed to generalize this conclusion. However, Zhang (2011) proposed valuable recommendations concerning the requisite simulation time for FPMD and the need to use multiple initial conditions. Increasing computational power should make it routine to carry out and establish confidence in such accurate simulations. FPMD simulations will eventually be the tool of choice for constraining the thermodynamic behaviour of multicomponent liquid solutions under extreme conditions of pressure and temperature, and the need for a strategy such as that presented here for interpolating among and making predictions from such simulations will become increasingly evident.

Modelling of systems that are subject to liquid-liquid immiscibility is not a simple matter. Indeed, as noted in this work, numerical modelling of liquid structure and properties is complicated by the tendency to unmix, in particular between the solvus and the spinodal where

the second liquid must nucleate before unmixing will take place, requiring calculation times potentially longer than those achievable with current computer resources.

Acknowledgements

We would like to thank Dr. James Sangster and Dr. Pierre Hudon for their constructive criticisms of the present work as well as the editors and reviewers at GCA for pushing us to improve the manuscript. This work was supported in part by Defence Research and Development Canada and by the US NSF through award EAR-1426526.

References

Ai, Y. and Lange, R.A. (2008) New acoustic velocity measurements on CaO-MgO-Al2O_3-SiO_2 liquids: Reevaluation of the volume and compressibility of $CaMgSi_2O_6$-$CaAl_2Si_2O_8$ liquids to 25 GPa. Journal of Geophysical Research: Solid Earth 113, B04203.

Alfè, D. (2005) Melting Curve of MgO from First-Principles Simulations. Physical Review Letters 94, 235701.

Asimow, P.D. and Ahrens, T.J. (2010) Shock compression of liquid silicates to 125 GPa: The anorthite-diopside join. Journal of Geophysical Research: Solid Earth 115, B10209.

Bale, C.W., Belisle, E., Chartrand, P., Decterov, S.A., Eriksson, G., Hack, K., Jung, I.H., Kang, Y.B., Melancon, J., Pelton, A.D., Robelin, C. and Petersen, S. (2009) FactSage thermochemical software and databases - recent developments. CALPHAD: Computer Coupling of Phase Diagrams and Thermochemistry 33, 295-311.

Belonoshko, A.B. and Dubrovinsky, L.S. (1996a) Molecular and lattice dynamics study of the MgO-SiO_2 system using a transferable interatomic potential. Geochim. Cosmochim. Acta 60, 1645-1656.

Belonoshko, A.B. and Dubrovinsky, L.S. (1996b) Molecular dynamics of NaCl (B1 and B2) and MgO (B1) melting: two-phase simulation. Am. Mineral. 81, 303-316.

Ben Martin, G., Ghiorso, M. and Spera, F.J. (2012) Transport properties and equation of state of 1-bar eutectic melt in the system $CaAl_2Si_2O8$-$CaMgSi_2O_6$ by molecular dynamics simulation. Am. Mineral. 97, 1155-1164.

Ben Martin, G., Spera, F.J., Ghiorso, M.S. and Nevins, D. (2009) Structure, thermodynamic, and transport properties of molten Mg_2SiO_4: molecular dynamics simulations and model EOS. Am. Mineral. 94, 693-703.

Benoit, M., Ispas, S., Jund, P. and Jullien, R. (2000) Model of silica glass from combined classical and ab initio molecular-dynamics simulations. Eur. Phys. J. B 13, 631-636.

Bottinga, Y., Weill, D.F., 1970. Densities of liquid silicate systems calculated from partial molar volumes of oxide components. Amer. J. Sci. 269, 169-182.

Bragg, W.L. and Williams, E.J. (1934) Effect of thermal agitation on atomic arrangement in alloys. Proceedings of the Royal Society of London, Series A: Mathematical, Physical and Engineering Sciences 145, 699-730.

Bragg, W.L. and Williams, E.J. (1935) Effect of thermal agitation on atomic arrangement in alloys. II. Proceedings of the Royal Society of London, Series A: Mathematical, Physical and Engineering Sciences 151, 540-566.

Carre, A., Horbach, J., Ispas, S. and Kob, W. (2008) New fitting scheme to obtain effective potential from Car-Parrinello molecular-dynamics simulations: application to silica. EPL 82, 17001/17001-17001/17006.
Courtial, P. and Dingwell, D.B. (1999) Densities of melts in the CaO-MgO-Al_2O_3-SiO_2 system. Am. Mineral. 84, 465-476.
Dalton, J.A. and Presnall, D.C. (1997) No liquid immiscibility in the system $MgSiO_3$-SiO_2 at 5.0 GPa. Geochimica et Cosmochimica Acta 61, 2367-2373.
Davies, G.F. (1973) Quasi-harmonic finite strain equations of state of solids. Journal of Physics and Chemistry of Solids 34, 1417-1429.
de Koker, N., Karki, B.B. and Stixrude, L. (2013) Thermodynamics of the MgO–SiO_2 liquid system in Earth's lowermost mantle from first principles. Earth and Planetary Science Letters 361, 58-63.
de Koker, N. and Stixrude, L. (2009) Self-consistent thermodynamic description of silicate liquids, with application to shock melting of MgO periclase and $MgSiO_3$ perovskite. Geophys. J. Int. 178, 162-179.
de Koker, N.P., Stixrude, L. and Karki, B.B. (2008) Thermodynamics, structure, dynamics, and freezing of Mg_2SiO_4 liquid at high pressure. Geochim. Cosmochim. Acta 72, 1427-1441.
Demiralp, E., Cagin, T. and Goddard, W.A., III (1999) Morse stretch potential charge equilibrium force field for ceramics: Application to the quartz-stishovite phase transition and to silica glass. Phys. Rev. Lett. 82, 1708-1711.
Fei, Y., Saxena, S.K. and Navrotsky, A. (1990) Internally consistent thermodynamic data and equilibrium phase relations for compounds in the system MgO-SiO_2 at high pressure and high temperature. Journal of Geophysical Research: Solid Earth 95, 6915-6928.
Feuston, B.P. and Garofalini, S.H. (1988) Empirical three-body potential for vitreous silica. Journal of Chemical Physics 89, 5818-5824.
Gheribi, A.E. (2009) Formulation of the thermal volume consistent with Swenson's concept of thermal pressure. Physics of the Earth and Planetary Interiors 177, 59-64.
Ghiorso, M.S. (2004a) An equation of state for silicate melts. I. Formulation of a general model. American Journal of Science 304, 637-678.
Ghiorso, M.S. (2004b) An equation of state for silicate melts. III. Analysis of stoichiometric liquids at elevated pressure: shock compression data, molecular dynamics simulations and mineral fusion curves. American Journal of Science 304, 752-810.
Ghiorso, M.S. (2004c) An equation of state for silicate melts. IV. Calibration of a multicomponent mixing model to 40 GPa. Am. J. Sci. 304, 811-838.
Ghiorso, M.S., Hirschmann, M.M., Reiners, P.W. and Kress, V.C. (2002) The pMELTS: A revision of MELTS for improved calculation of phase relations and major element partitioning related to partial melting of the mantle to 3 GPa. Geochemistry, Geophysics, Geosystems 3, 1-35.
Ghiorso, M.S. and Kress, V.C. (2004) An equation of state for silicate melts. II. Calibration of volumetric properties at 105 Pa. Am. J. Sci. 304, 679-751.
Ghiorso, M., Sack, R., 1995. Chemical mass transfer in magmatic processes IV. A revised and internally consistent thermodynamic model for the interpolation and extrapolation of liquid-solid equilibria in magmatic systems at elevated temperatures and pressures. Contrib. Mineral. Petrol. 119, 197-212.
Grundy, A.N., Jung, I.-H., Pelton, A.D. and Decterov, S.A. (2008a) A model to calculate the viscosity of silicate melts: part II: the $NaO_{0.5}$-MgO-CaO-$AlO_{1.5}$-SiO_2 system. International Journal of Materials Research 99, 1195-1209.
Grundy, A.N., Liu, H., Jung, I.-H., Decterov, S.A. and Pelton, A.D. (2008b) A model to calculate the viscosity of silicate melts: part I: viscosity of binary SiO_2-MeOx systems (Me = Na, K, Ca, Mg, Al). International Journal of Materials Research 99, 1185-1194.
Guillot, B. and Sator, N. (2007) A computer simulation study of natural silicate melts. Part II: High pressure properties. Geochimica et Cosmochimica Acta 71, 4538-4556.

Hageman, V.B.M. and Oonk, H.A.J. (1986) Liquid immiscibility in the SiO2 + MgO, SiO_2 + SrO, SiO_2 + La_2O_3, and SiO_2 + Y_2O_3 systems. Phys. Chem. Glasses 27, 194-198.
Harvey, J.P., Asimow, P.D. (2015) Current limitations of molecular dynamic simulations as probes of thermo-physical behavior of silicate melts, in press.
Harvey, J.P., Gheribi, A.E. and Chartrand, P. (2011) Accurate determination of the Gibbs energy of Cu-Zr melts using the thermodynamic integration method in Monte Carlo simulations. Journal of Chemical Physics 135, 084502/084501-084502/084513.
Harvey, J.P., Gheribi, A.E. and Chartrand, P. (2012) Thermodynamic integration based on classical atomistic simulations to determine the Gibbs energy of condensed phases: Calculation of the aluminum-zirconium system. Physical Review B 86, 224202.
Hassanali, A.A. and Singer, S.J. (2007) Model for the Water-Amorphous Silica Interface: The Undissociated Surface. J. Phys. Chem. B 111, 11181-11193.
Herzbach, D., Binder, K. and Müser, M.H. (2005) Comparison of model potentials for molecular-dynamics simulations of silica. The Journal of Chemical Physics 123, -.
Holland, T. and Powell, R. (2003) Activity–composition relations for phases in petrological calculations: an asymmetric multicomponent formulation. Contrib Mineral Petrol 145, 492-501.
Hovis, G.L., Toplis, M.J., Richet, P. (2004) Thermodynamic mixing properties of sodium silicate liquids and implications for liquid–liquid immiscibility. Chemical Geology 213, 173-186.
Hudon, P. and Baker, D.R. (2002a) The nature of phase separation in binary oxide melts and glasses. I. Silicate systems. J. Non-Cryst. Solids 303, 299-345.
Hudon, P. and Baker, D.R. (2002b) The nature of phase separation in binary oxide melts and glasses. II. Selective solution mechanism. J. Non-Cryst. Solids 303, 346-353.
Hudon, P., Baker, D.R., Pelton, A.D. and Wu, P. (1994) Disappearance of the Liquid-Liquid Miscibility Gap in the System CaO-MgO-SiO_2 at High Pressure. Mineralogical Magazine 58A, 434-435.
Hudon, P., Jung, I.-H. and Baker, D.R. (2002) Melting of β-quartz up to 2.0 GPa and thermodynamic optimization of the silica liquidus up to 6.0 GPa. Physics of the Earth and Planetary Interiors 130, 159-174.
Hudon, P., Jung, I.-H. and Baker, D.R. (2004) Effect of pressure on liquid-liquid miscibility gaps: a case study of the systems CaO-SiO2, MgO-SiO_2, and $CaMgSi_2O_6$-SiO_2. J. Geophys. Res., [Solid Earth] 109, B03207/03201-B03207/03218.
Hudon, P., Jung, I.-H. and Baker, D.R. (2005) Experimental investigation and optimization of thermodynamic properties and phase diagrams in the systems CaO-SiO_2, MgO-SiO_2, $CaMgSi_2O_6$-SiO_2, and $CaMgSi_2O_6$-Mg_2SiO_4 to 1.0 GPa. J. Petrol. 46, 1859-1880.
Jacobs, M.H.G. and Oonk, H.A.J. (2000) A new equation of state based on Grover, Getting and Kennedy's empirical relation between volume and bulk modulus. The high-pressure thermodynamics of MgO. Physical Chemistry Chemical Physics 2, 2641-2646.
Kambayashi, S. and Kato, E. (1983) A thermodynamic study of (magnesium oxide + silicon dioxide) by mass spectrometry. J. Chem. Thermodyn. 15, 701-707.
Kambayashi, S. and Kato, E. (1984) A thermodynamic study of magnesium oxide + silicon dioxide by mass spectrometry at 1973 K. J. Chem. Thermodyn. 16, 241-248.
Karki, B.B., Zhang, J., Stixrude, L. (2013) First principles viscosity and derived models for MgO-SiO2 melt system at high temperature. Geophysical Research Letters 40, 94-99.
Karki, B.B., Bhattarai, D. and Stixrude, L. (2006) First-principles calculations of the structural, dynamical, and electronic properties of liquid MgO. Physical Review B 73, 174208.
Karki, B.B., Bhattarai, D. and Stixrude, L. (2007) First-principles simulations of liquid silica: Structural and dynamical behavior at high pressure. Physical Review B 76, 104205.
Kikuchi, R. (1951) A theory of cooperative phenomena. Physical Review 81, 988-1003.

Lacks, D.J., Rear, D.B. and Van Orman, J.A. (2007) Molecular dynamics investigation of viscosity, chemical diffusivities and partial molar volumes of liquids along the $MgO–SiO_2$ join as functions of pressure. Geochimica et Cosmochimica Acta 71, 1312-1323.

Lange, R.A. (1997) A revised model for the density and thermal expansivity of K_2O-Na_2O-CaO-MgO-Al_2O_3-SiO_2 liquids from 700 to 1900 K: extension to crustal magmatic temperatures. Contrib Mineral Petrol 130, 1-11.

Leu, A.-L., Ma, S.-M. and Eyring, H. (1975) Properties of Molten Magnesium Oxide. Proceedings of the National Academy of Sciences 72, 1026-1030.

Liu, Z.-J., Cheng, X.-L., Zhang, H. and Cai, L.-C. (2004) Molecular dynamics study for the melting curve of MgO at high pressure. Chin. Phys. (Beijing, China) 13, 384-387.

Matsui, M., Parker, S.C. and Leslie, M. (2000) The MD simulation of the equation of state of MgO: application as a pressure calibration standard at high temperature and high pressure. Am. Mineral. 85, 312-316.

Mitra, S.K., Amini, M., Fincham, D. and Hockney, R.W. (1981) Molecular dynamics simulation of silicon dioxide glass. Philosophical Magazine Part B 43, 365-372.

Oganov, A.R., Brodholt, J.P. and David Price, G. (2000) Comparative study of quasiharmonic lattice dynamics, molecular dynamics and Debye model applied to $MgSiO_3$ perovskite. Physics of the Earth and Planetary Interiors 122, 277-288.

Ol'shanskii, Y.I. (1951) Equilibria of two immiscible liquids in systems of alkaline earth silicates. Dokl. Akad. Nauk SSSR 76, 93-96.

Paduraru, A., Kenoufi, A., Bailey, N.P. and Schioetz, J. (2007) An interatomic potential for studying CuZr bulk metallic glasses. Advanced Engineering Materials 9, 505-508.

Paramore, S., Cheng, L. and Berne, B.J. (2008) A Systematic Comparison of Pairwise and Many-Body Silica Potentials. J. Chem. Theory Comput. 4, 1698-1708.

Pelton, A.D. and Blander, M. (1986) Thermodynamic analysis of ordered liquid solutions by a modified quasichemical approach-application to silicate slags. Metall. Trans. B 17B, 805-815.

Pelton, A.D., Chartrand, P. and Eriksson, G. (2001) The modified quasi-chemical model: Part IV. Two-sublattice quadruplet approximation. Metall. Mater. Trans. A 32, 1409-1416.

Pelton, A.D., Degterov, S.A., Eriksson, G., Robelin, C. and Dessureault, Y. (2000) The modified quasichemical model I - binary solutions. Metallurgical and Materials Transactions B: Process Metallurgy and Materials Processing Science 31B, 651-659.

Pelton, A.D. and Kang, Y.-B. (2007) Modeling short-range ordering in solutions. International Journal of Materials Research 98, 907-917.

Rein, R.H. and Chipman, J. (1965) Activities in the liquid solution SiO_2-CaO-MgO-Al_2O_3 at 1600°. Trans. Am. Inst. Min., Metall. Pet. Eng. 233, 415-425.

Rivers, M.L. and Carmichael, I.S.E. (1987) Ultrasonic studies of silicate melts. Journal of Geophysical Research: Solid Earth 92, 9247-9270.

Robelin, C., Chartrand, P. and Eriksson, G. (2007) A Density Model for Multicomponent Liquids Based on the Modified Quasichemical Model: Application to the NaCl-KCl-$MgCl_2$-$CaCl_2$ System. Metall and Materi Trans B 38, 869-879.

Rustad, J.R., Yuen, D.A. and Spera, F.J. (1991) The sensitivity of physical and spectral properties of silica glass to variations of interatomic potentials under high pressure. Physics of the Earth and Planetary Interiors 65, 210-230.

Soules, T.F. (1990) Computer simulation of glass structures. J. Non-Cryst. Solids 123, 48-70.

Soules, T.F., Gilmer, G.H., Matthews, M.J., Stolken, J.S. and Feit, M.D. (2011) Silica molecular dynamic force fields—A practical assessment. Journal of Non-Crystalline Solids 357, 1564-1573.

Spera, F.J., Ghiorso, M.S. and Nevins, D. (2011) Structure, thermodynamic and transport properties of liquid $MgSiO_3$: Comparison of molecular models and laboratory results. Geochim. Cosmochim. Acta 75, 1272-1296.

Spera, F.J., Nevins, D., Ghiorso, M. and Cutler, I. (2009) Structure, thermodynamic and transport properties of $CaAl_2Si_2O8$ liquid. Part I: Molecular dynamics simulations. Geochim. Cosmochim. Acta 73, 6918-6936.

Takada, A., Richet, P., Catlow, C.R.A. and Price, G.D. (2004) Molecular dynamics simulations of vitreous silica structures. Journal of Non-Crystalline Solids 345–346, 224-229.

Tangney, P. and Scandolo, S. (2002) An ab initio parametrized interatomic force field for silica. Journal of Chemical Physics 117, 8898-8904.

Tsuneyuki, S., Tsukada, M., Aoki, H. and Matsui, Y. (1988) First-principles interatomic potential of silica applied to molecular dynamics. Phys. Rev. Lett. 61, 869-872.

Vashishta, P., Kalia, R.K., Rino, J.P. and Ebbsjoe, I. (1990) Interaction potential for silica: a molecular-dynamics study of structural correlations. Phys. Rev. B: Condens. Matter 41, 12197-12209.

Wasserman, E.A., Yuen, D.A. and Rustad, J.R. (1993) Compositional effects on the transport and thermodynamic properties of MgO-SiO_2 mixtures using molecular dynamics. Physics of the Earth and Planetary Interiors 77, 189-203.

Woodcock, L.V., Angell, C.A. and Cheeseman, P. (1976) Molecular dynamics studies of the vitreous state: Simple ionic systems and silica. Journal of Chemical Physics 65, 1565-1577.

Wu, P., Eriksson, G., Pelton, A.D. and Blander, M. (1993) Prediction of the Thermodynamic Properties and Phase Diagrams of Silicate Systems -- Evaluation of the FeO-MgO-SiO_2 System. ISIJ International 33, 26-35.

Yang, C.N. (1945) Generalization of the quasi-chemical method in the statistical theory of superlattices. Journal of Chemical Physics 13, 66-76.

Zaitsev, A.I. and Mogutnov, B.M. (1997) Thermodynamics of CaO-SiO_2 and MnO-SiO_2 melts: II. Thermodynamic modeling and phase-equilibrium calculations. Inorg. Mater. (Transl. of Neorg. Mater.) 33, 823-831.

Zerr, A. and Boehler, R. (1994) Constraints on the melting temperature of the lower mantle from high-pressure experiments on MgO and magnesioustite. Nature 371, 506-508.

Zhang, L. (2011) Thermodynamic properties calculation for MgO-SiO_2 liquids using both empirical and first-principles molecular simulations. Physical Chemistry Chemical Physics 13, 21009-21015.

Appendix 1: Classical thermodynamic description of the thermo-physical properties of multicomponent liquid solutions

The total Gibbs energy of a multicomponent solution $G^{solution}\left(T,P,\underline{X}\right)$ is typically defined by the following equation:

$$G^{solution}\left(T,P,\underline{X}\right)=\sum_{i=1}^{s}n_i\cdot g_i^0\left(T,P\right)-T\Delta S^{config.}\left(T,P,\underline{X}\right)+G^{xs,non-config.}\left(T,P,\underline{X}\right) \quad \text{(A1-1)}$$

In eq. A1-1, n_i and $g_i^0\left(T,P\right)$ are the number of moles and the standard molar Gibbs energy of species *i* respectively; $\Delta S^{config.}\left(T,P,\underline{X}\right)$ is the total configurational entropy of mixing and $G^{xs,non-config.}\left(T,P,\underline{X}\right)$ is the total non-configurational excess Gibbs energy induced by the mixing of the *s* species. This last term in eq. A1-1 is a collection of all potential non-ideal and non-configurational contributions to the Gibbs energy (harmonic, anharmonic, lattice vacancies for solid solutions, magnetism, electronic, pressure, etc.). The Gibbs energy of a solution depends on the temperature *T*, the pressure *P*, and chemical composition in the form of a vector: $\underline{X}=\left[X_1,X_2,...,X_s\right]$, where X_i is the molar fraction of the i^{th} species.

If we define the total Gibbs energy of mixing $\Delta G^{mix.}\left(T,P,\underline{X}\right)$ as:

$$\Delta G^{mix.}\left(T,P,\underline{X}\right)\equiv G^{solution}\left(T,P,\underline{X}\right)-\sum_{i=1}^{s}n_i\cdot g_i^0\left(T,P\right) \quad \text{(A1-2)}$$

then an alternative general expression for $\Delta G^{mix.}\left(T,P,\underline{X}\right)$, independent of the pure species terms, can be obtained:

$$\Delta G^{mix.}\left(T,P,\underline{X}\right)=-T\Delta S_{P_0}^{config.}\left(T,\underline{X}\right)+G^{xs}\left(T,P,\underline{X}\right) \quad \text{(A1-3)}$$

Note that in eq. A1-3, the pressure dependence of the configurational entropy of mixing has been incorporated into a global excess Gibbs energy function defined as $G^{xs}\left(T,P,\underline{X}\right)$. In other words, the total excess volume will be defined as a sum of configurational-dependent and configurational-independent contributions. In theory, the distinction between these two contributions can be formulated if both volumetric and structural data are available.

Taking atmospheric pressure P_0 as the reference state pressure for describing the thermodynamic behaviour of the solution, $\Delta G^{mix.}\left(T,P,\underline{X}\right)$ can then be redefined as a function of the excess Gibbs energy of mixing at P_0, $G^{xs}_{P_0}\left(T,\underline{X}\right)$, and an excess Gibbs energy contribution for changing the pressure from P_0 to P, a function defined as $\Delta G^{xs}_{P_0\to P}\left(T,P,\underline{X}\right)$, as follows:

$$\Delta G^{mix.}\left(T,P,\underline{X}\right)=-T\Delta S^{config.}_{P_0}\left(T,\underline{X}\right)+G^{xs}_{P_0}\left(T,\underline{X}\right)+\Delta G^{xs}_{P_0\to P}\left(T,P,\underline{X}\right) \qquad \text{(A1-4)}$$

In this work, $G^{xs}_{P_0}\left(T,\underline{X}\right)$, $\Delta S^{config.}_{P_0}\left(T,\underline{X}\right)$ and $\Delta G^{xs}_{P_0\to P}\left(T,P,\underline{X}\right)$ can all be expressed as a function of species molar fractions, but can also be a function of species equivalent fractions, pair fractions, quadruplet fractions, etc., depending on the thermodynamic model used to describe the energetic behaviour of the solution. In eq. A1-4, $\Delta G^{xs}_{P_0\to P}\left(T,P,\underline{X}\right)$ is the energetic contribution related to the work associated with the excess volume v^{xs} of the solution upon change in pressure from P_0 to P.

As proposed in our definition of $G^{solution}\left(T,P,\underline{X}\right)$, the configurational entropy of mixing can be potentially an implicit function of both pressure and temperature. This is a direct consequence of the possible dependence of species populations on these variables. Several approximations are available in the literature to describe the configurational entropy of mixing. The judicious selection of the model depends on the chemical nature of the solution considered. For multicomponent systems with weak chemical interactions between the pure species, the ideal solution approximation, also called the Bragg-Williams random-mixing model for solid solutions (Bragg and Williams, 1934, 1935), is used:

$$\Delta S^{config.}_{ideal}=-R\cdot\sum_{i=1}^{s}n_i\ln\left(X_i\right) \qquad \text{(A1-5)}$$

In this case the configurational entropy of mixing is a function of neither *T* nor *P*. A similar expression to eq. A1-5 is used when covalent or ionic bonds between atoms lead to the formation of structural entities (often called associates) that are weakly interacting in the solution.

For other complex solutions presenting chemical interactions between these two limiting cases, such as silicate melts, a more complex mathematical expression for the configurational entropy of mixing has to be used. In this case, the limitation in eq. A1-5 is alleviated by the addition of purely empirical excess parameters to eq. A1-1. For solid solutions, the cluster variation method (Kikuchi, 1951) is often used to describe both the short range order (SRO) and long range chemical order (LRO). In this model, the higher geometrical entity that defines the species of the solution is determined by the symmetry of the solid structure to be modelled. For liquid solutions, quasichemical approaches (Pelton and Blander, 1986; Pelton *et al.*, 2001; Pelton *et al.*, 2000; Yang, 1945) are often considered in order to define the configurational entropy of mixing since they take account of SRO.

The selection of an adequate thermodynamic model for silicate melts is not simple. The main reason for this is the presence, in pure liquid silica at low pressure, of a three-dimensional network formed by SiO_4 tetrahedra linked together by bridging oxygen (the silicon coordination is close to 4 in these conditions). Molecular dynamic simulations of silica glass (Rustad *et al.*, 1991) show that it gradually becomes a compact liquid at high pressure with the silicon cation-anion coordination number ranging from 5 to 8. When adding a network modifier such as CaO or MgO to pure liquid silica, the three-dimensional network is rapidly destroyed. This can be seen in viscosity measurements (see Grundy *et al.* (2008a, 2008b)). The total number of configurations with the same internal energy, which defines the total entropy of the system, increases drastically as more free SiO_4 tetrahedra are present in the solution upon destruction of bridging oxygen bonds. The destruction of this three-dimensional symmetry in silica-rich melts and its direct impact on the configurational entropy of mixing is difficult to model even approximately. Several investigators have tried to estimate the configurational entropy of mixing of silicate melts by adding expressions similar to eq. A1-5 for cation distributions in different coordination states (de Koker *et al.*, 2013) or for monomeric, associated complexes and polymeric molecules (Zaitsev and Mogutnov, 1997). However, it has to be remembered that eq. A1-5 is valid only for random distribution of distinct species on a lattice presenting the same

number of equivalent sites, in other words assuming no chemical interactions between the distinct species. In this case, the configurational entropy of mixing per mole of sites cannot exceed the ideal entropy. When entities or species are destroyed upon mixing, then the total number of entities in the system increases, leading to potentially higher entropy of mixing per mole of sites compared to the ideal entropy expression. However, if the resulting entropy of mixing is referred per (g-atom), then it would have again to be smaller than the ideal entropy of mixing value.

Appendix 2: Thermodynamic excess properties derived from v^{xs} functional forms

A. Polynomial representation

Thermodynamic excess properties of the excess volume function presented in section III-A are defined as follows:

$$\Delta g^{xs}_{P_0\to P}\left(T,P,\underline{X}\right)=Y_1Y_2\sum_{i+j\geq 0}\left[\sum_{q\geq 0}\left[l_{ij}^{q}+k_{ij}^{q}\cdot T\right]\frac{\left(P-P_0\right)^{q+1}}{q+1}\right]Y_1^{i}Y_2^{j} \tag{A2-1}$$

$$\Delta s^{xs}_{P_0\to P}=-\frac{\partial\left[\Delta g^{xs}_{P_0\to P}\left(T,P,\underline{X}\right)\right]}{\partial T}=Y_1Y_2\sum_{i+j\geq 0}\left[\sum_{q\geq 0}-k_{ij}^{q}\frac{\left(P-P_0\right)^{q+1}}{q+1}\right]Y_1^{i}Y_2^{j} \tag{A2-2}$$

$$\Delta h^{xs}_{P_0\to P}=-T^2\frac{\partial\left[\Delta g^{xs}_{P_0\to P}\left(T,P,\underline{X}\right)/T\right]}{\partial T}=Y_1Y_2\sum_{i+j\geq 0}\left[\sum_{q\geq 0}l_{ij}^{q}\frac{\left(P-P_0\right)^{q+1}}{q+1}\right]Y_1^{i}Y_2^{j} \tag{A2-3}$$

According to these equations, a simultaneous fit of $\Delta h^{mix.}\left(T,P,\underline{X}\right)$ and $v^{xs}\left(T,P,\underline{X}\right)$ is sufficient to allow the complete parameterization of $\Delta g^{xs}_{P_0\to P}\left(T,P,\underline{X}\right)$.

B. Exponential representation

Thermodynamic excess properties of the excess volume function presented in section III-B are defined as follows:

$$\Delta g^{xs}_{P_0\to P}\left(T,P,\underline{X}\right)=Y_1Y_2\sum_{i+j\geq 0}\left[\begin{array}{l}\dfrac{\left[a_{ij}d_{ij}+b_{ij}d_{ij}T+c_{ij}d_{ij}\left(P-P_0\right)-c_{ij}\right]}{{d_{ij}}^2}exp\left[d_{ij}\left(P-P_0\right)+f_{ij}T\right]\\ -\dfrac{\left[a_{ij}d_{ij}+b_{ij}d_{ij}T-c_{ij}\right]}{{d_{ij}}^2}exp\left[f_{ij}T\right]\end{array}\right]Y_1^iY_2^j \tag{A2-4}$$

$$\Delta s^{xs}_{P_0\to P}\left(T,P,\underline{X}\right)=Y_1Y_2\sum_{i+j\geq 0}\left[\begin{array}{l}-\dfrac{\left[\begin{array}{l}f_{ij}\left[d_{ij}\left(a_{ij}+b_{ij}T+c_{ij}\left(P-P_0\right)\right)-c_{ij}\right]\\ +b_{ij}d_{ij}\end{array}\right]}{{d_{ij}}^2}\cdot exp\left[d_{ij}\left(P-P_0\right)+f_{ij}T\right]\\ +\dfrac{\left[\begin{array}{l}f_{ij}\left[d_{ij}\left(a_{ij}+b_{ij}T\right)-c_{ij}\right]\\ +b_{ij}d_{ij}\end{array}\right]}{{d_{ij}}^2}\cdot exp\left[f_{ij}T\right]\end{array}\right]Y_1^iY_2^j \tag{A2-5}$$

$$\Delta h^{xs}_{P_0\to P}\left(T,P,\underline{X}\right)=Y_1Y_2\sum_{i+j\geq 0}\left[\begin{array}{l}-\dfrac{\left[\begin{array}{l}f_{ij}\cdot d_{ij}\cdot T\left[a_{ij}+b_{ij}T+c_{ij}\left(P-P_0\right)\right]\\ -c_{ij}\,f_{ij}T-a_{ij}d_{ij}-c_{ij}d_{ij}\left(P-P_0\right)+c_{ij}\end{array}\right]}{{d_{ij}}^2}\cdot exp\left[d_{ij}\left(P-P_0\right)+f_{ij}T\right]\\ +\dfrac{\left[\begin{array}{l}f_{ij}\cdot d_{ij}\cdot T\left[a_{ij}+b_{ij}T\right]-c_{ij}\,f_{ij}T-a_{ij}d_{ij}+c_{ij}\end{array}\right]}{{d_{ij}}^2}\cdot exp\left[f_{ij}T\right]\end{array}\right]Y_1^iY_2^j \tag{A2-6}$$

$$\Gamma^{xs}\left(T,P,\underline{X}\right)=Y_1Y_2\sum_{i+j\geq 0}\left[\left[d_{ij}\left(a_{ij}+b_{ij}T+c_{ij}\left(P-P_0\right)\right)+c_{ij}\right]\cdot exp\left[d_{ij}\left(P-P_0\right)+f_{ij}T\right]\right]Y_1^iY_2^j \tag{A2-7}$$

$$\Omega^{xs}\left(T,P,\underline{X}\right)=Y_1Y_2\sum_{i+j\geq 0}\left[\left[f_{ij}\left(a_{ij}+b_{ij}T+c_{ij}\left(P-P_0\right)\right)+b_{ij}\right]\cdot exp\left[d_{ij}\left(P-P_0\right)+f_{ij}T\right]\right]Y_1^iY_2^j \tag{A2-8}$$

Appendix 3: Parameterization of the excess volume functions

In this appendix, we present the optimal parameters $(\beta_{00}, \beta_{70}, \omega_{00}, \omega_{70})$ of eqs. 24 and 25 used to reproduce raw FPMD simulation data of de Koker *et al.* 2013.

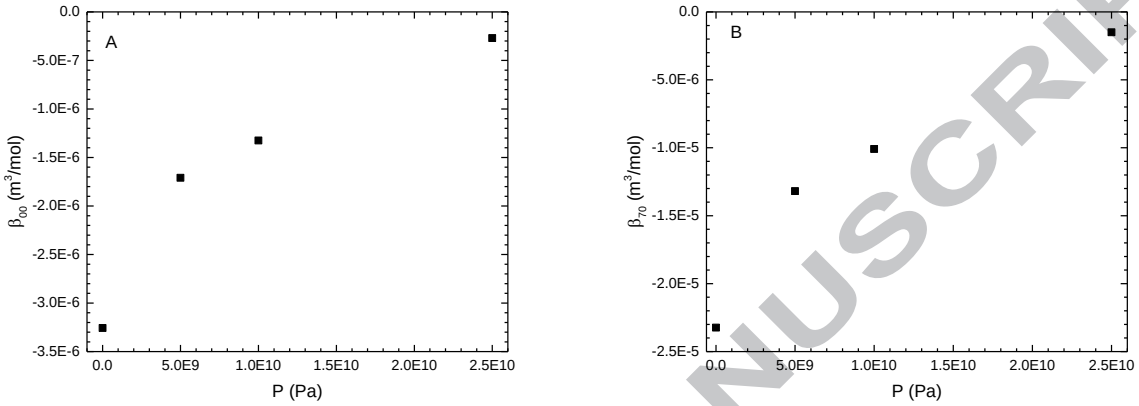

Figure A- 1: Parameters of eq. 24 defining $\left(\frac{v^{xs}}{z_{tot.}/2}\right)$ for different pressures, A) β_{00}, B) β_{70}

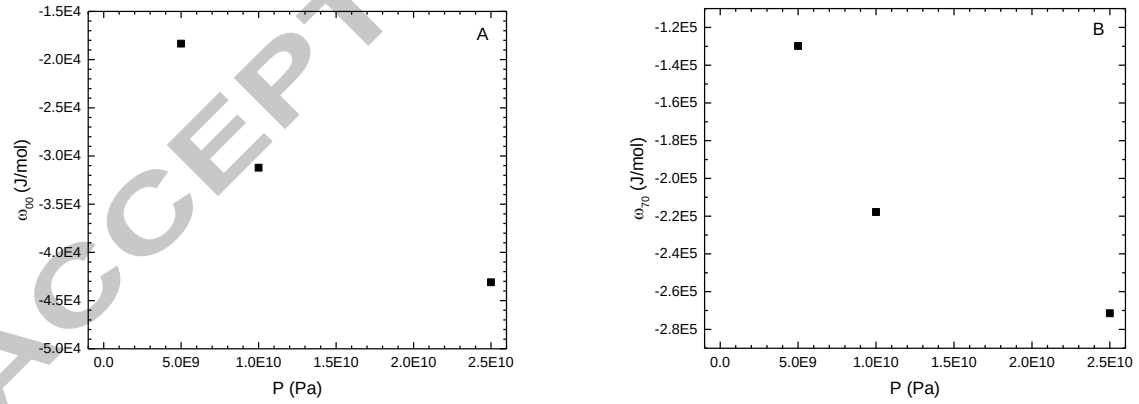

Figure A- 2: Parameters of eq. 25 defining $\left(\frac{\Delta h_P^{xs} - h_{P_0}^{xs}}{z_{tot.}/2}\right)$ for different pressures; A) ω_{00}, B) ω_{70}

Appendix 4: Gibbs energy functions of the MgO-periclase (B1) and the MgO-liquid phase as a function of temperature up to 5000 K and 25 GPa

MgO crystallizes in the B1 (Fm3m) structure and is commonly designated as periclase. The Gibbs energy of periclase was formulated in a prior work (Gheribi, 2009) up to 160 GPa. It was shown that the bulk modulus increases linearly with pressure up to 160 GPa, and consequently that the Murnaghan EOS is suitable to describe the pressure dependence of the Gibbs energy. The consistency of the formulation was verified. No anomalous behaviour of the pressure dependence of the heat capacity or entropy were observed, which can happen when an unsuitable EOS is chosen to describe the Gibbs energy (Jacobs and Oonk, 2000).

The Gibbs energy of MgO liquid as a function of temperature at standard pressure was taken from the FTOxide database in FactSage (Bale *et al.*, 2009). The EOS describing the pressure dependence of the Gibbs energy of liquid MgO is not available in the literature. The formulation of the EOS of liquid MgO is a difficult task since no experimental data on the P-V-T curve or physical properties directly linked to the EOS (density, thermal expansion, bulk modulus and its pressure derivative) are available. In recent years, classical and FPMD simulations were performed in order to estimate the EOS of liquid MgO (Alfè, 2005; Belonoshko and Dubrovinsky, 1996b; Liu *et al.*, 2004). Leu *et al.* (Leu et al., 1975) estimated the thermo-physical properties of liquid MgO from statistical thermodynamics based on a suitable partition function. Other studies (Ai and Lange, 2008; Courtial and Dingwell, 1999; Ghiorso, 2004c; Ghiorso and Kress, 2004; Rivers and Carmichael, 1987) attempted to estimate the thermo-physical properties of liquid MgO based on the thermo-physical properties of multicomponent liquids using advanced interpolation techniques.

In this work, we aim to formulate the Gibbs energy of liquid MgO up to 25 GPa in order to estimate the liquidus temperature of the MgO-SiO_2 system in the SiO_2-rich side at 5 GPa. We assume that, like the solid, the Murnaghan EOS is suitable for describing the pressure dependence of the Gibbs energy of the liquid phase at least up to 25 GPa (i.e. we assume that, in this pressure range, the bulk modulus of the liquid phase also increases linearly with pressure).

The temperature-dependent Murnaghan EOS is expressed as follows:

$$V(T,P)=V(T_0,P_0)e^{\int_{T_0}^{T}\alpha_V(T,P_0)dT}\left\{1+P\left[\frac{B_T^{'}(T,P_0)}{B_T(T,P_0)}\right]\right\}^{\frac{-1}{B_T^{'}(T,P_0)}} \quad \text{(A4-1)}$$

The parameterization procedure of the EOS follows a similar strategy to that of Paduraru *et al.* (2007). The target parameters are those determined by Leu *et al.* (1975) and are optimized in order to minimize simultaneously the quadratic error on the melting curve of MgO and the EOS at 3000 K obtained from classical molecular dynamic simulations (Lacks *et al.*, 2007). The choice of classical MD data instead of FPMD data is not arbitrary. The empirical potentials of Lacks *et al.* (2007) for this system are formulated based on experimental data for solid MgO and reproduce the energetic interactions of the solid phase with good accuracy.

Results of the optimization procedure for eq. A4-1 are as follows:

$$\begin{cases} T_0 = 3000\,K \\ V(T_0,P_0) = 16.2\cdot10^{-6}\,m^3 \\ \alpha_V(T,P_0) = 1.5\cdot10^{-4}\,K^{-1} \\ B_T(T,P_0) = \left[25.96-0.0107\cdot(T-T_0)\right]\cdot10^9\,Pa \\ B_T^{'}(T,P_0) = 4.8 \end{cases} \quad \text{(A4-2)}$$

As pointed out by Ghiorso (2004a), eq. A4-2 should be used with care as it can potentially lead to unphysical properties (i.e. a negative bulk modulus) at high temperature and low pressure. In this specific case, eq. A4-2 is applicable up to 5425K. Above this temperature, an unphysical behavior of liquid MgO will be predicted by this EOS. The optimized melting curve and isothermal EOS at 3000 K are shown in Fig. A-3 and Fig. A-4 respectively.

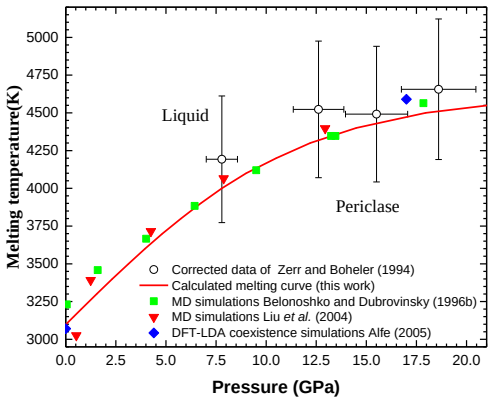

Figure A- 3: Calculated melting curve of MgO obtained from the Gibbs energy of periclase formulated by Gheribi (2009) and the Gibbs energy of the liquid phase formulated in this work. The calculated P-T curve is compared with the corrected experimental data of Zerr an Boehler (1994) corrected by Liu et al. (2004) (open cricles) and of various classical molecular dynamics (squares: Belonoshko and Dubrovinski (Belonoshko and Dubrovinsky, 1996b) data; inverted triangles: Liu *et al.* (2004)) and FPMD simulations (diamonds: Alfè (2005)).

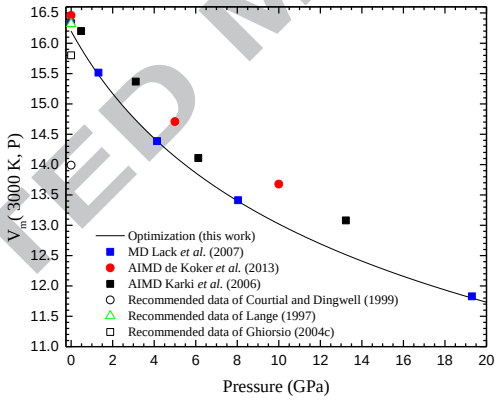

Figure A- 4: Calculated EOS of the liquid MgO at 3000 K compared with the MD simulations of Lacks *et al.* (2007) and the FPMD simulations data of de Koker *et al.* (2013) and Karki *et al.* (2006) Recommended values of V_o based on multicomponent system fitting by Courtial and Dingwell (1999) (open circles), Lange (1997) and Ghiorso (2004c) are (open squares) are also shown.

In the optimization procedure, we have adjusted $V\left(T_0, P_0\right)$ and $\alpha_V\left(T, P_0\right)$ to 16.2*10^{-6}m and 1.5*10^{-4} K^{-1} in comparison with the work of Leu *et al.* (1975) while using the same isothermal

bulk modulus as reported by these authors. The optimized thermal expansion of $1.5*10^{-4}$ K^{-1} is very close to the suggested values of Ghiorso (2004c) and of Lange (1997). The Grüneisen parameter deduced from the present optimized physical properties is equal to 1.15 and the calculated sound velocity is 3950 m s^{-1}.